Supporting information for

Application of a ferrocene-chelating heteroscorpionate ligand in nickel mediated radical polymerization

Shuangshuang Li,[a, b] Ashton R. Davis,[c] Hootan Roshandel,[c] Nima Adhami,[c] Yi Shen,[c] Nathalie H. Co,[c] Leo A. Morag,[c] Hafez Etemad,[c] Yuan Liu,[b] Paula L. Diaconescu[c, *]

[a] College of Chemistry and Pharmaceutical Sciences, Qingdao Agricultural University, Qingdao 266109, China
[b] Department of Catalysis Science and Technology, School of Chemical Engineering, Tianjin University, Tianjin 300350, China
[c] Department of Chemistry and Biochemistry, University of California, Los Angeles 607 Charles E. Young Drive East, Los Angeles CA 90095, USA
*E-mail: pld@chem.ucla.edu

Table of Contents

Table S1. Control homopolymerization reactions.

| Entry	Condition[a]	Monomer[b]	Time (h)	T (°C)	Conv. (%)	Mn_{calc} (kg/mol)[c]	Mn_{exp} (kg/mol)[d]	$Đ$[d]
1	**red**	styrene	24	80	26	N/D[e]	N/D[e]	N/D[e]
2	**ox**	styrene	0.1	RT	98	N/D[e]	N/D[e]	N/D[e]
3	**red**	p-CS	24	80	87	N/D[e]	N/D[e]	N/D[e]
4	**ox**	p-CS	24	RT	>99	N/D[e]	N/D[e]	N/D[e]
5	**red**	MMA	24	80	NR	-	-	-
6	**ox**	MMA	24	RT	NR	-	-	-
7	**red**	n-BuMA	24	80	NR	-	-	-
8	**ox**	n-BuMA	24	RT	NR	-	-	-
9	**red**	acrylonitrile	24	80	NR	-	-	-
10	**ox**	acrylonitrile	24	RT	NR	-	-	-
11	**oxi**	styrene	24	RT	NR	-	-	-
12	**oxi**	p-CS	24	RT	NR	-	-	-
13	**oxi**	MMA	24	RT	NR	-	-	-
14	**oxi**	n-BuMA	24	RT	NR	-	-	-
15	**red**	MMA	22	RT	NR	-	-	-
16	**red**	acrylonitrile	24	RT	NR	-	-	-

Conditions: monomer (1.05 mmol), 1, 3, 5-trimethoxybenzene (TMB) as an internal standard (0.1167 mmol), FcBAr^F as the oxidant (0.0111 mmol), and C$_6$D$_6$ and o-difluorobenzene as the solvent (a total volume of 0.5 mL); [a] "**red**" and "**ox**" refer to the reduced and *in situ* generated oxidized compound (fc^{P,B})NiBr (0.0111 mmol) in the absence of ethyl 2-bromoisobutyrate, "**oxi**" refers to experiments with FcBAr^F and ethyl 2-bromoisobutyrate (0.0111 mmol) but no (fc^{P,B})NiBr. [b] p-CS = p-chlorostyrene, MMA = methyl methacrylate, n-BuMA = n-butyl methacrylate. [c] Determined by ^{1}H NMR spectroscopy. [d] Determined by SEC. [e] Not determined, polymer could not be isolated suggesting formation of oligomers.

Table S2. Failed copolymerization attempts using (fc^{P,B})NiBr and its oxidized counterpart.

Entry	Monomer 1[a]	Monomer 2	Monomer 3	Catalyst[b]	Time (h)	Conv. (%)
1	styrene	n-BuMA	/	**ox-red**	0.2-42	99-62
2	n-BuMA	styrene	/	**red-ox**	22-2.5	86-99
3	p-CS	MMA	/	**red-ox**	46-22	96-0
4	n-BuMA	MMA	/	**red-ox**	22-28	86-75
5	styrene	p-CS	styrene	**ox-red-ox**	0.2-46-24	99-18-92

Conditions: monomer (1.05 mmol), ethyl 2-bromoisobutyrate (0.0111 mmol), (fc^{P,B})NiBr (0.0111 mmol), (1, 3, 5-trimethoxybenzene (TMB) as an internal standard (0.1167 mmol), FcBAr^F as oxidant (0.0111 mmol), CoCp$_2$ as reductant (0.0111 mmol), and C$_6$D$_6$ and difluorobenzene as solvent. Reaction temperatures were based on homopolymer studies, unless otherwise mentioned. [a] n-BuMA = n-butyl methacrylate, MMA = methyl methacrylate, p-CS = p-chlorostyrene [b] "**red**" and "**ox**" refer to the reduced and *in situ* generated oxidized compound.

Conversion plots
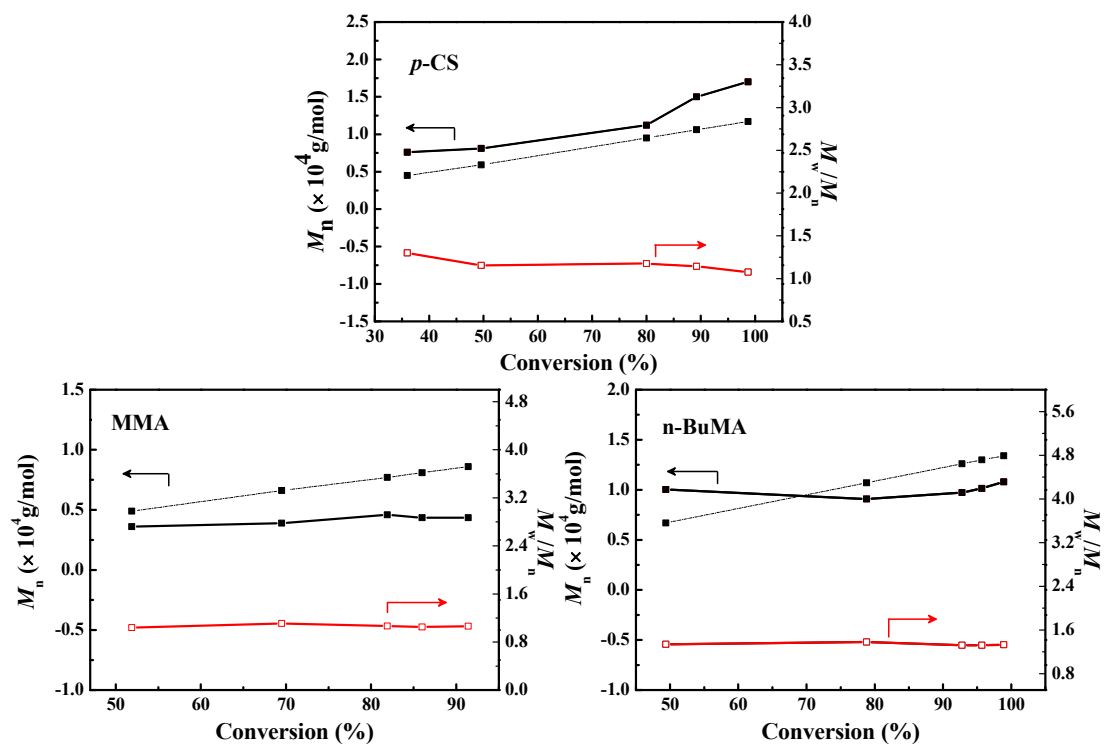
Figure S1. Conversion dependence of M_n and M_w/M_n for *p*-CS, MMA, and *n*-BuMA polymerization with (fc^{P,B})NiBr or [(fc^{P,B})NiBr][BAr^F]. The black lines use the y axis at left and red line with right, as the arrows indicate; the dotted line is for the theoretical M_n.
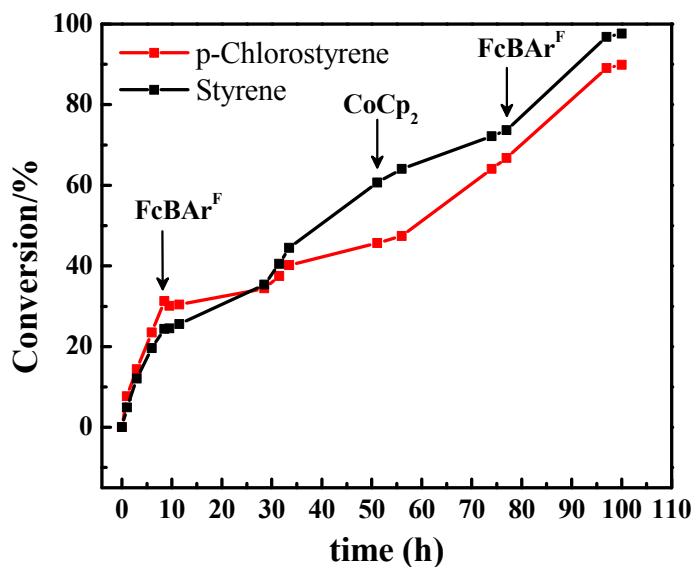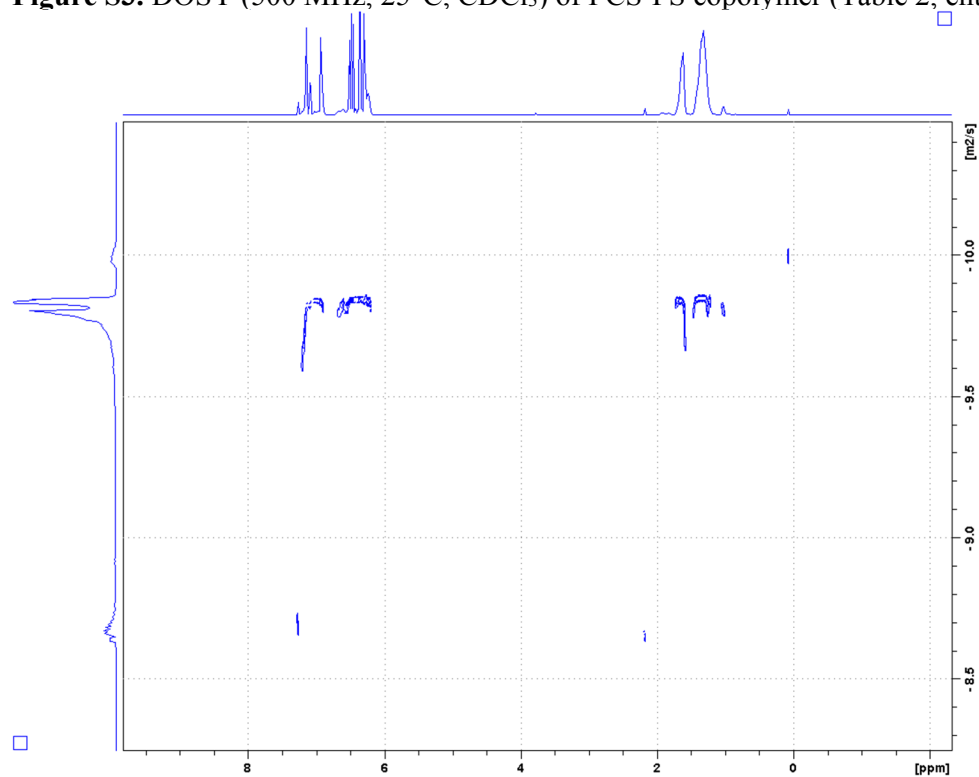

Figure S2. Plot of conversion (%) vs time for the polymerization of styrene and p-CS by one-pot with (fc^{P,B})NiBr using *in situ* oxidation and reduction with FcBAr^F and CoCp$_2$, respectively.
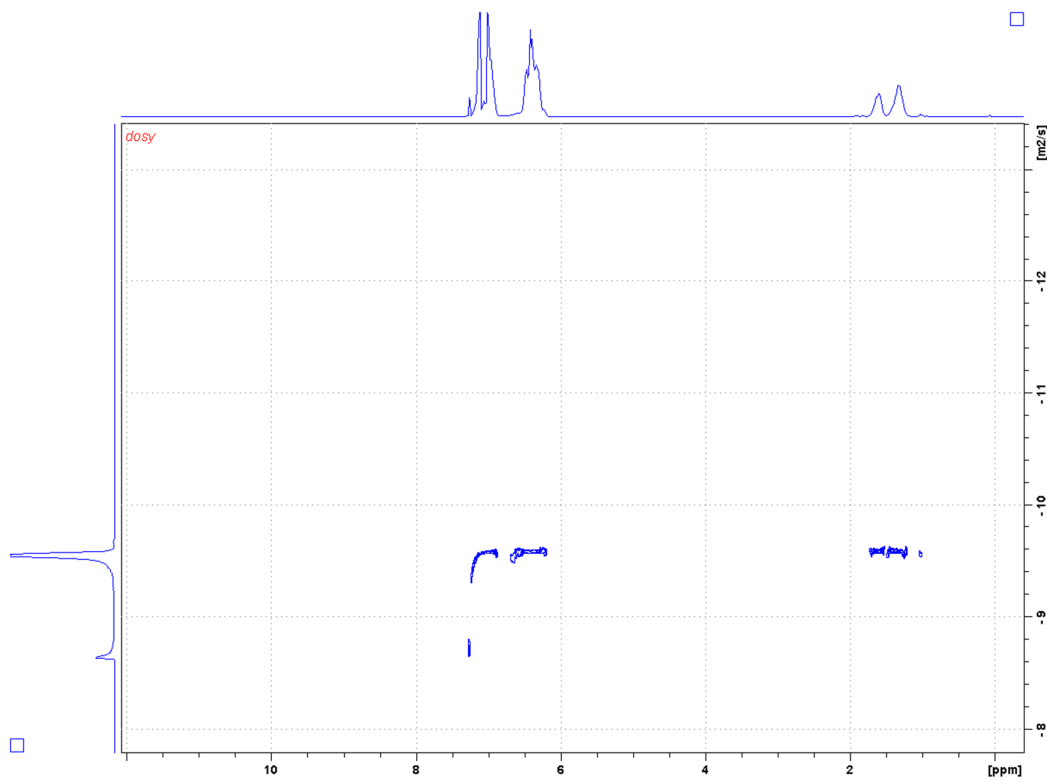
DOSY
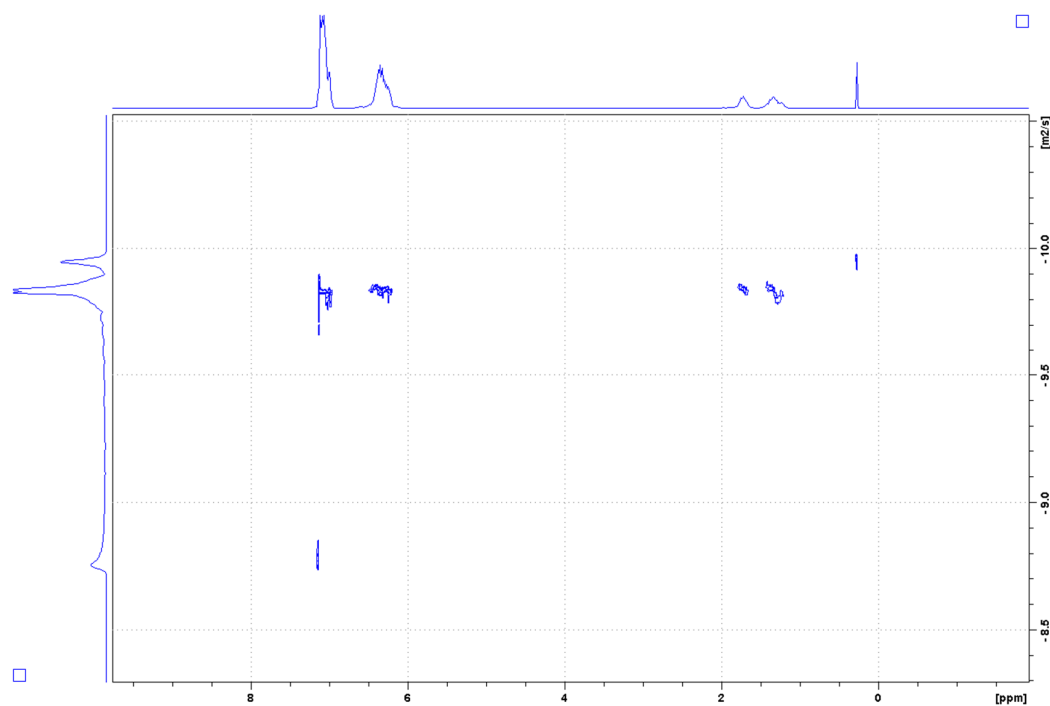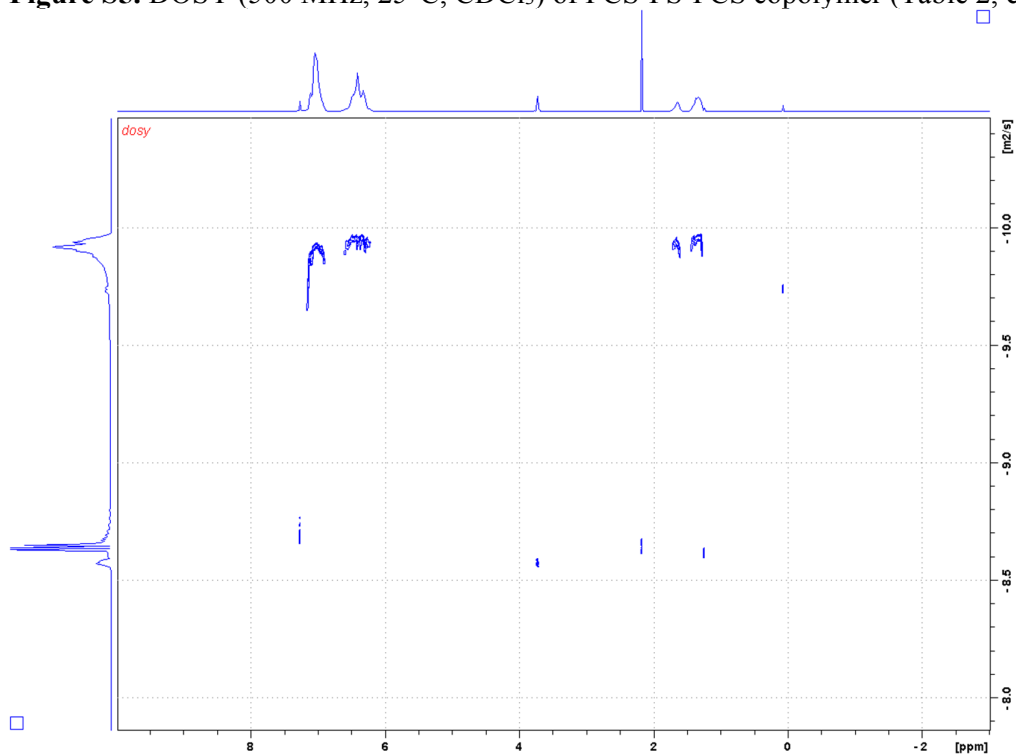

Figure S3. DOSY (500 MHz, 25°C, CDCl₃) of PCS-PS copolymer (Table 2, entry 2).

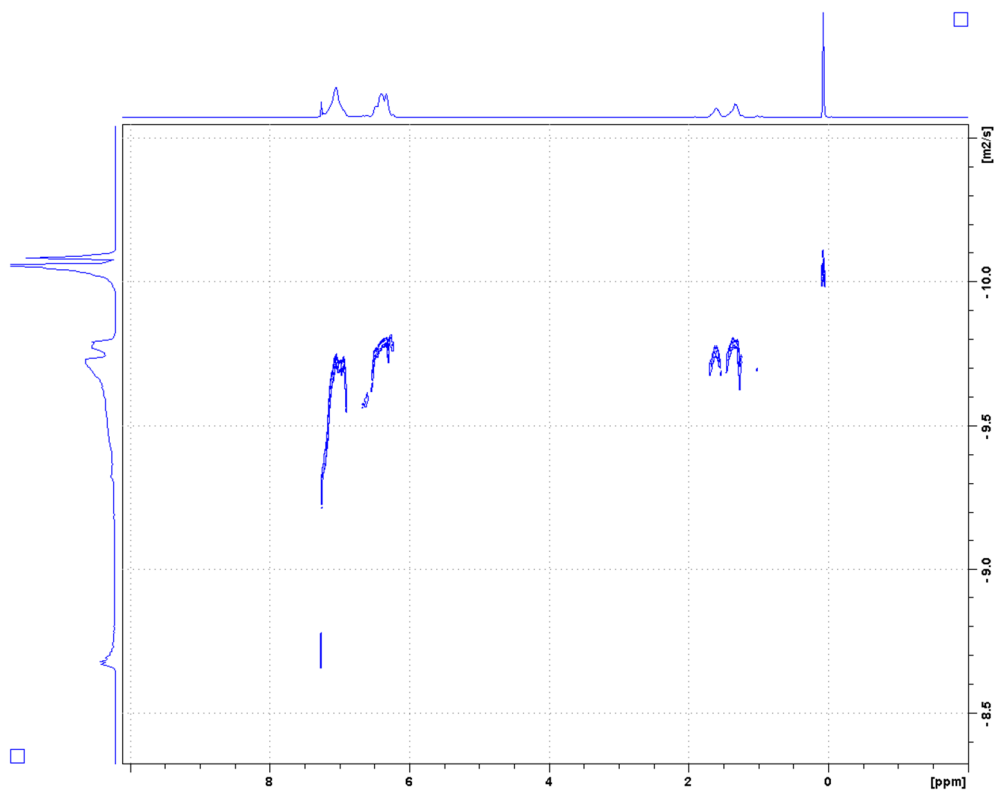
Figure S4. DOSY (500 MHz, 25°C, CDCl₃) of PS-PCS copolymer (Table 2, entry 4).

**Figure S5.** DOSY (500 MHz, 25°C, CDCl₃) of PCS-PS-PCS copolymer (Table 2, entry 5).

**Figure S6.** DOSY (500 MHz, 25°C, CDCl₃) of PS-PCS-PS copolymer (Table S2, entry 5).

Figure S7. DOSY (500 MHz, 25°C, CDCl₃) of a mixture of PCS and PS homopolymers.

Stejskal-Tanner plots

Stejskal-Tanner plots are derived from diffusion ordered spectroscopy (DOSY) NMR experiments.[1] These plots show the decay of signal intensity versus the gradient applied over the course of the experiment. The rate of signal decay is unique to each molecule in the sample, and as such Stejskal-Tanner plots offer a convenient method to test whether a polymer sample is a mixture of homopolymers or a true copolymer. In a copolymer, the signal from both polymerized monomers will have equivalent intensity decay across all gradients whereas a mixture of homopolymers will show different intensity decays.
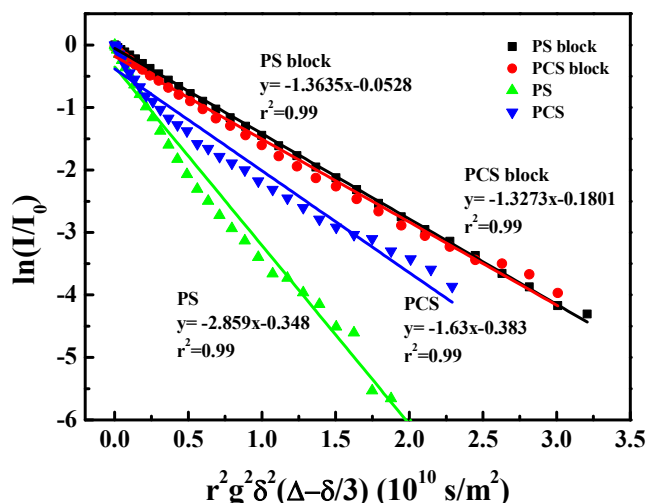

Figure S8. Stejskal-Tanner plot of the diffusion activity of the PS and PCS blocks in PS-PCS copolymer compared to the PS and PCS homopolymers (Table 2, entries 1-3).
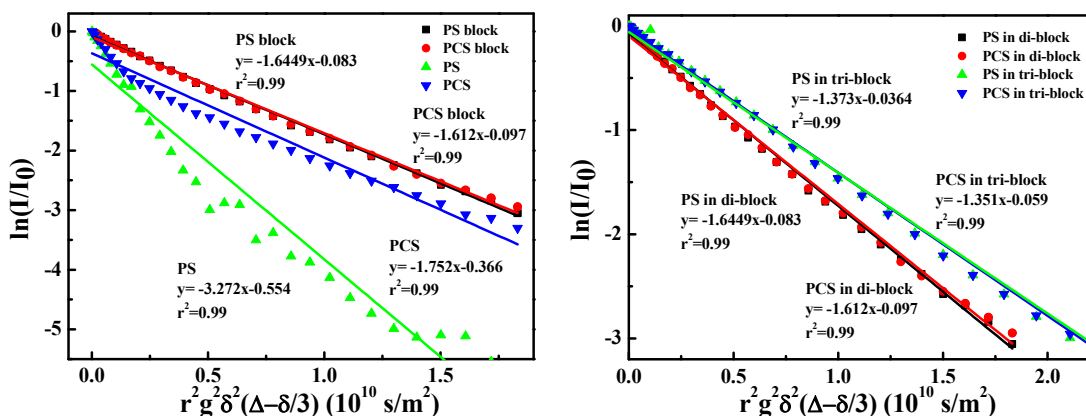
Figure S9. Stejskal-Tanner plot of the diffusion activity of the PCS and PS blocks in a PCS-PS copolymer compared to PCS and PS homopolymers (left) and of the diffusion activity of the PCS and PS blocks in PCS-PS-PCS compared to those blocks in PCS-PS (right).
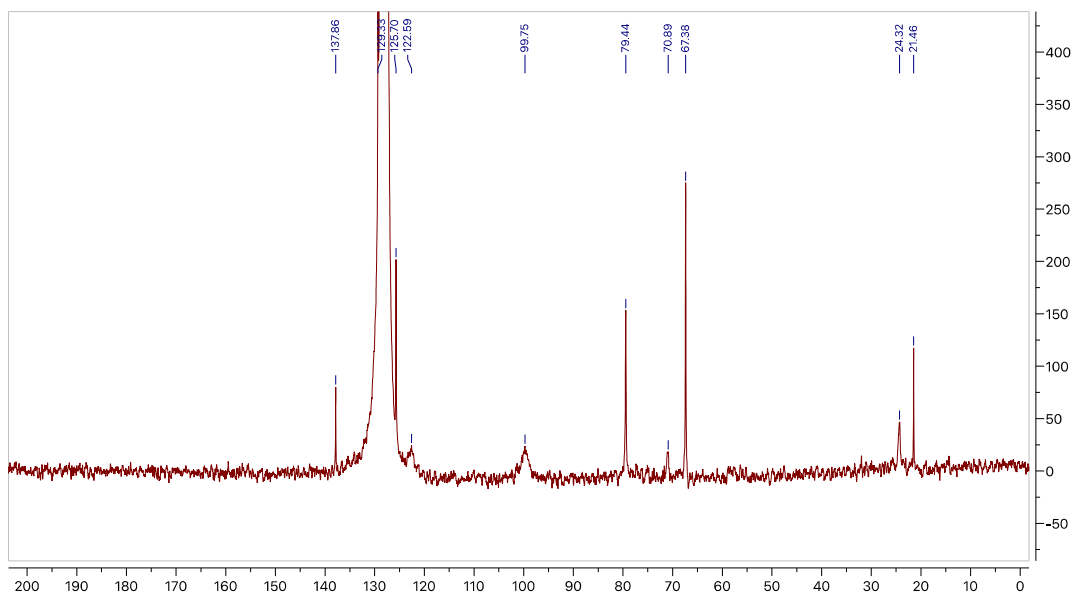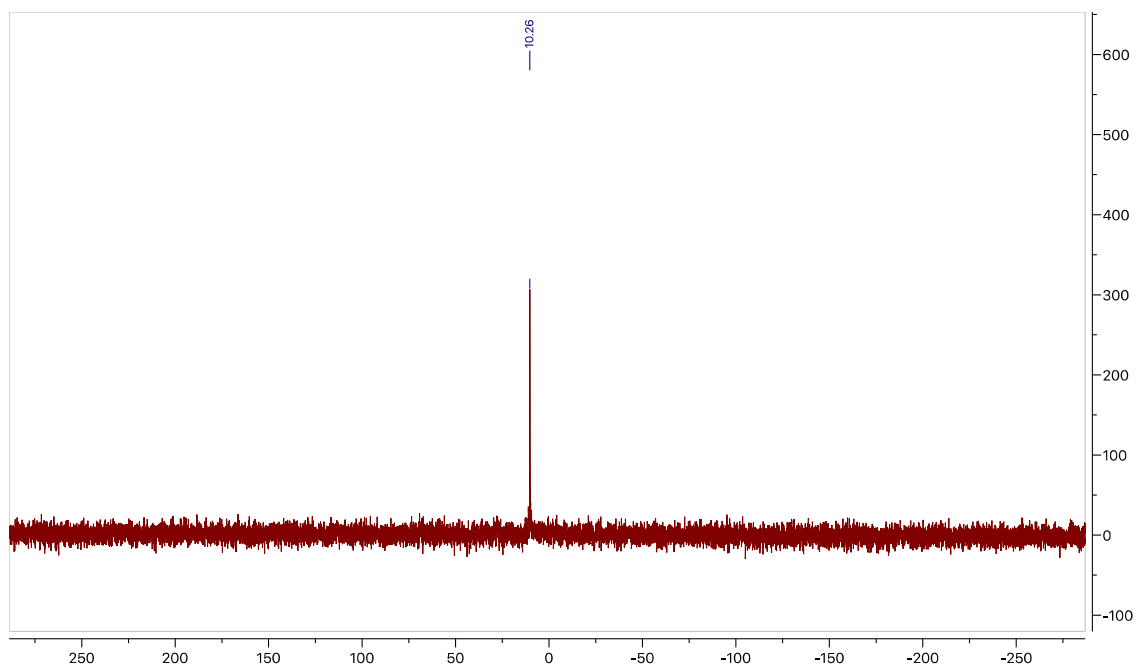
NMR spectra
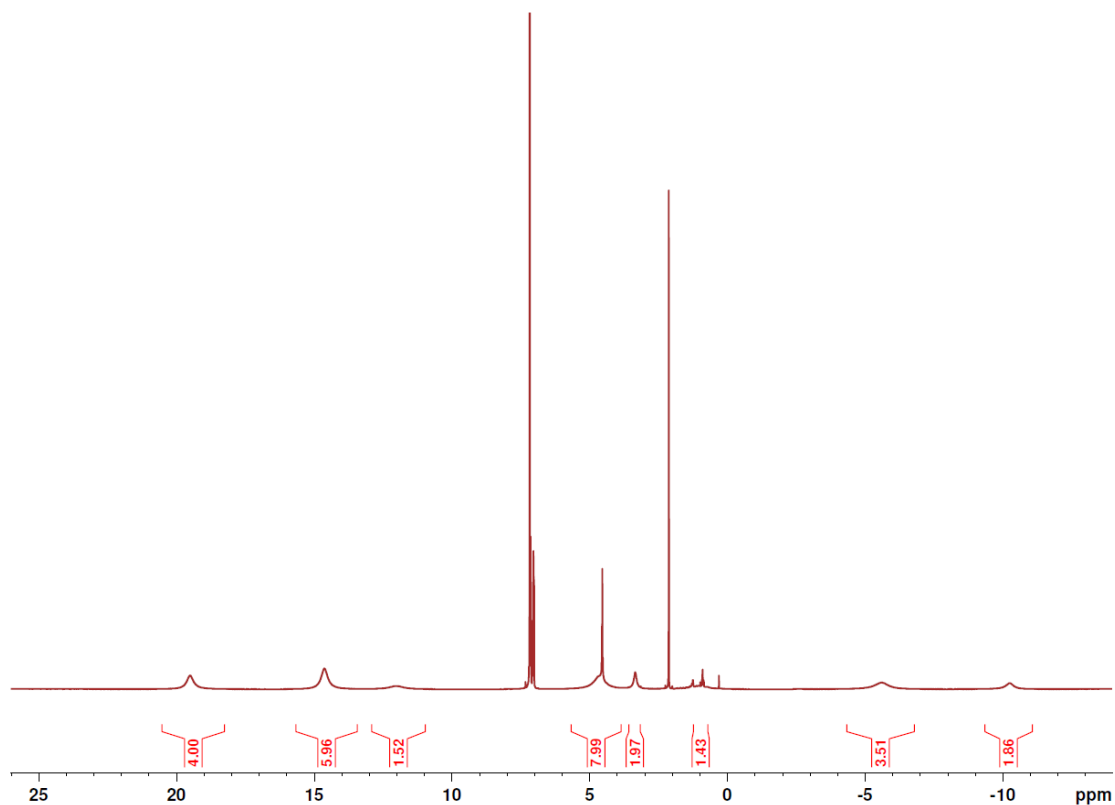
Figure S10. ^{1}H NMR (500 MHz, 25 °C, C$_6$D$_6$) spectrum of (fc^{P,B})NiBr·(C$_7$H$_8$). δ (ppm): 19.50 (s,br, 4H, *o*-ArH), 14.62 (s, br, 6H, *m,p*-ArH), 12.02 (s, br, 1H, pyrazole-H), 4.55(s, br, 6H, Cp-H), 4.53(s, 3H, pyrazole-CH$_3$), 3.34 (s, br, 2H, Cp-H), 0.98 (s, br, 1H, pyrazole-H), -5.61 (s, br, 3H, pyrazole-CH$_3$), -10.26 (s, br, 1H, pyrazole-H). Peaks at 7.13 ppm, 7.02 ppm, and 2.11 ppm are attributed to residual toluene.

Note: The ^{1}H NMR spectrum of (fc^{P,B})NiBr·(C$_7$H$_8$) corresponds to the previously reported ^{1}H NMR spectrum of (fc^{P,B})NiCl·(C$_7$H$_8$).[2]

Figure S11. ^{13}C NMR spectrum (126 MHz, 25 °C, C_6D_6) of (fc^{P,B})NiBr: δ (ppm) 125.70 (s, aromatic) 122.59 (s, br, aromatic), 99.75(s, br, CH), 79.44 (s, Cp-*C*), 70.89 (s, br, Cp-*C*), 67.38 (s, Cp-*C*), 24.32 (s, br, C*C*H₃). Peaks at 137.86 ppm, 129.33 ppm, 125.70, and 21.46 ppm are attributed to residual toluene.

Figure S12. ^{31}P NMR spectrum (121 MHz, 25 °C, C_6D_6) spectrum of (fc^{P,B})NiBr: δ (ppm) 10.26 (s).

9
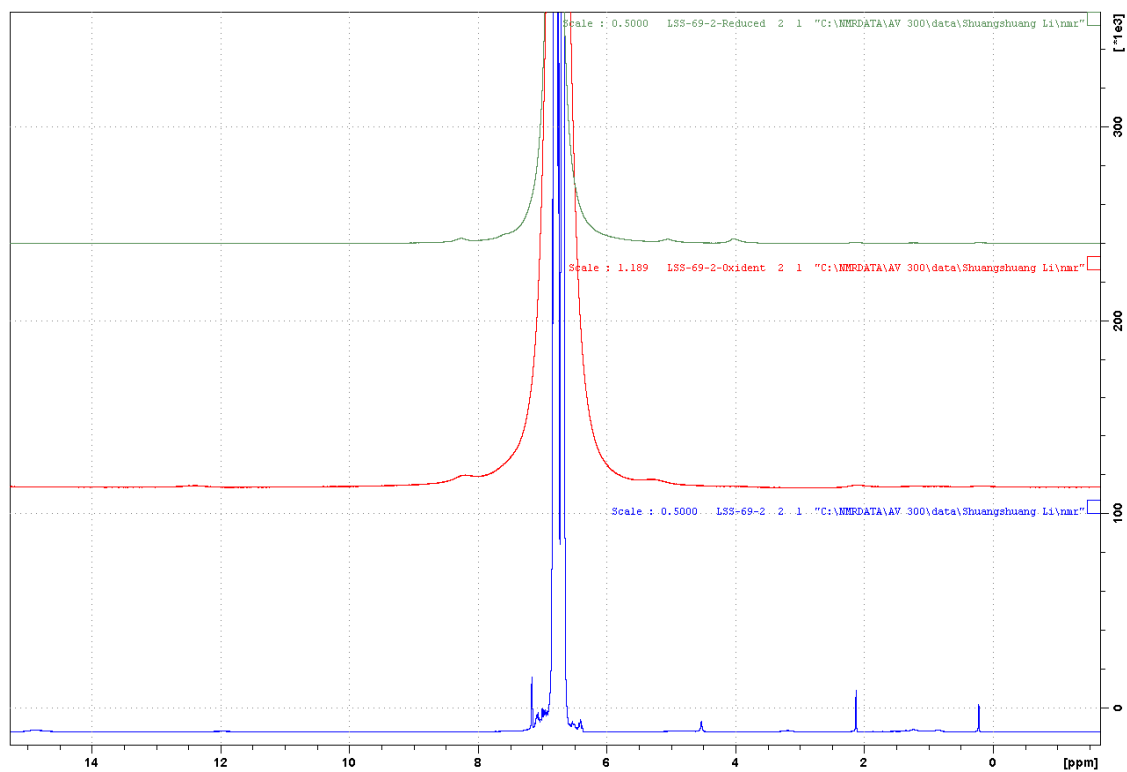
Figure S13. ^{1}H NMR (300 MHz, 25 °C, C$_6$D$_6$) spectrum of *in situ* redox switching of (fc^{P,B})NiBr. We have (fc^{P,B})NiBr (bottom), [(fc^{P,B})NiBr][BAr^F] after adding oxidant FcBAr^F (middle), and regenerated (fc^{P,B})NiBr after adding reductant CoCp$_2$ (top).
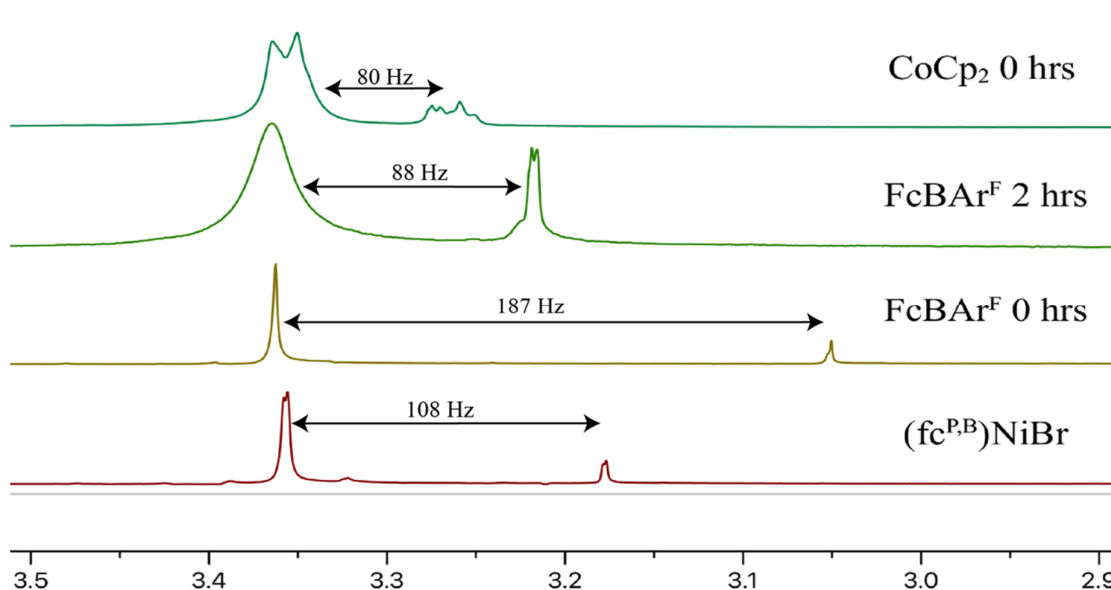
Figure S14. ^1H NMR (600 MHz, 25°C, 1:1 DFB:C_6D_6) solution state magnetic susceptibility study of chemical redox switching of $(fc^{P,B})NiBr$. Referenced using 5% (w/v) TMB solution in 1:1 DFB:C_6D_6 (5 mg of compound in 0.5 mL of total solvent). δ (ppm): 3.36 (s, 3H, OCH_3, TMB inside sealed capillary) 3.25-3.04 (s, 3H, OCH_3, TMB in solution with $(fc^{P,B})NiBr$).

The chemical shifts in Figure S14 where used to calculate the molar magnetic susceptibility by employing the following equation:

$$\chi_M = \frac{3\Delta f}{4\pi Fc}$$

Where Δf is the chemical shift change in Hz, F is the spectrometer radiofrequency in Hz, and c is the concentration in mol/mL. The magnetic susceptibility values can then be used to calculate the effective magnetic moment of the system using:

$$\mu_{eff} = \sqrt{8\chi_M T}$$

Where T is the temperature in K. The calculated magnetic moments are then compared to theoretical μ values calculated from n number of unpaired electrons using:

$$\mu_{eff} = \sqrt{n(n+2)}$$

Table S3. Results of the Evans method with $(fc^{P,B})NiBr$ compounds.

Entry	Compound	Calculated μ_{eff}	Number of unpaired electrons
1	$(fc^{P,B})NiBr$	2.70	2
2	$[(fc^{P,B})NiBr]^+$ (0 hr)	3.55	3
3	$[(fc^{P,B})NiBr]^+$ (2 hr)	2.43	2
4	$(fc^{P,B})NiBr$	2.32	2
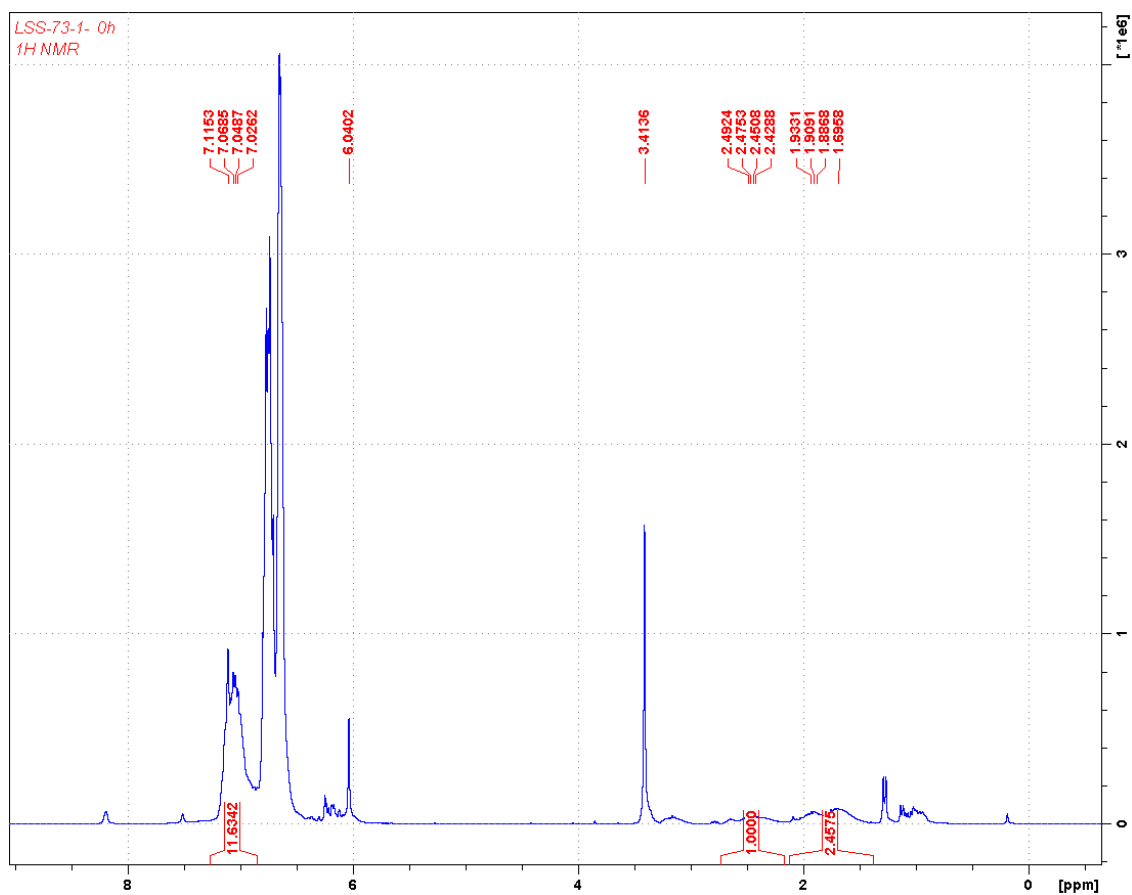
Figure S15. ^{1}H NMR (500 MHz, 25°C, C$_6$D$_6$) spectrum of 100 equivalents of styrene polymerization by [(fc^{P,B})NiBr][BAr^F] (Table 1, entry 2). δ (ppm): 7.02 (m, 5H, ArH, PS), 6.46-6.85 (m, 4H, 1,2-difluorobenzene), 6.04 (s, 3H, TMB), 3.41 (s, 9H, OCH$_3$, TMB), 2.45 (br t, 1H, C*H*CH$_2$, PS), 1.88 (br d, 2H, CHC*H$_2$*, PS).
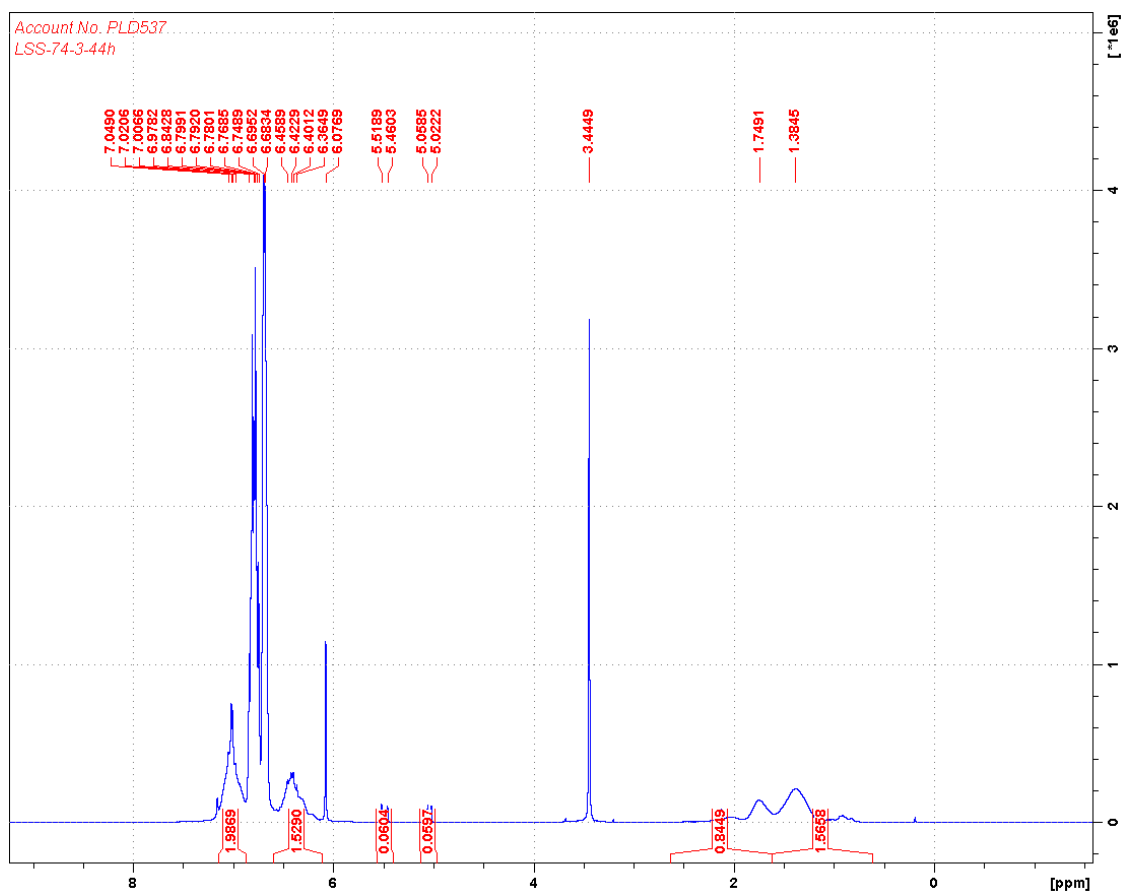
Figure S16. ^{1}H NMR (500 MHz, 25°C, C_6D_6) spectrum of 100 equivalents of *p*-chlorostyrene polymerization by (fc[P,B])NiBr (Table 1, entry 4). δ (ppm): 7.02 (m, 2H, ArH, PCS), 6.58-6.89 (m, 4H, 1,2-difluorobenzene), 6.42 (m, 2H, ArH, PCS), 6.07 (s, 3H, TMB), 5.50 (d, 1H, CHC*H*2, p-CS), 5.05 (d, 1H, CHC*H*2, p-CS), 3.44 (s, 9H, OCH3, TMB), 1.75 (br t, 1H, C*H*CH2, PCS), 1.38 (br d, 2H, CHC*H*2, PCS).
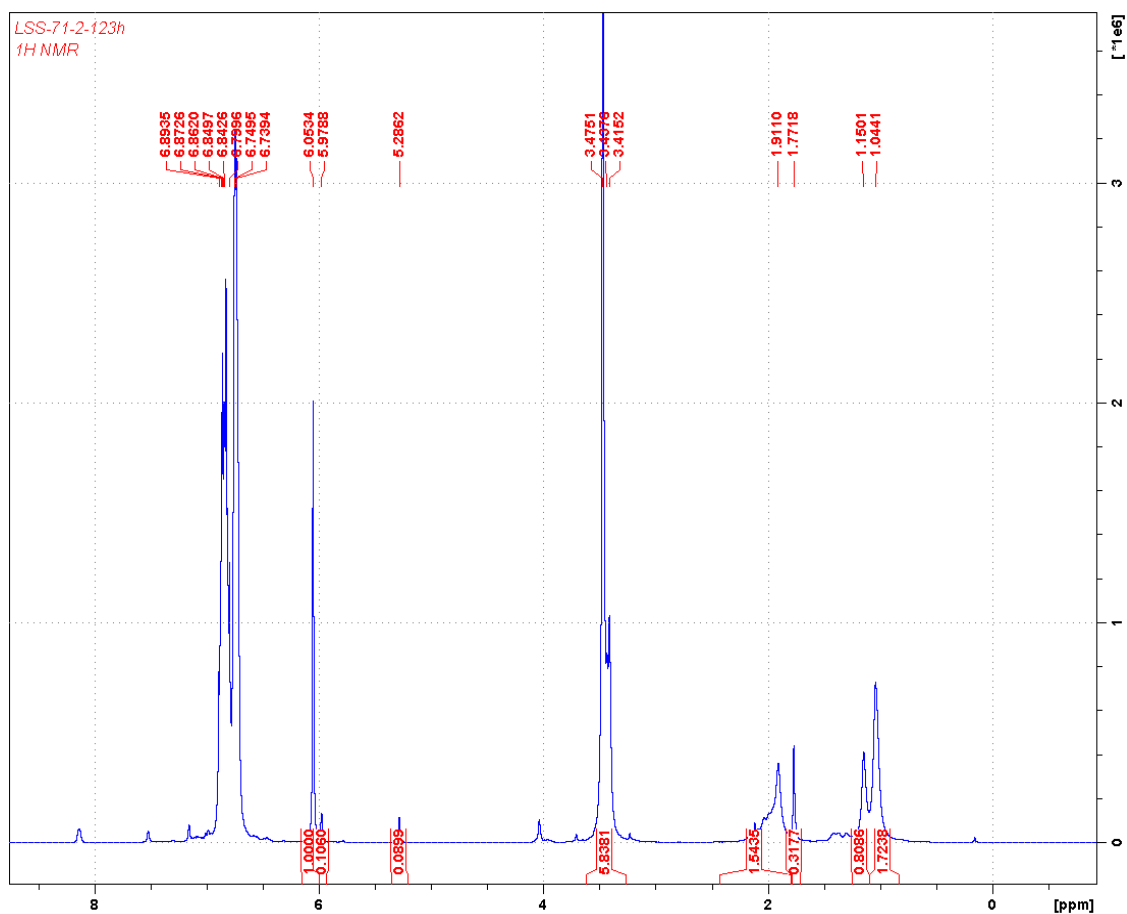
Figure S17. ^{1}H NMR (500 MHz, 25°C, C$_6$D$_6$) spectrum of 100 equivalents of methyl methacrylate polymerization by [(fc^{P,B})NiBr][BAr^F] (Table 1, entry 6). δ (ppm): 6.53-6.89 (m, 4H, 1,2-difluorobenzene), 6.05 (s, 3H, TMB), 5.98 (s, 1H, C*H*$_2$CCH$_3$, MMA), 5.29 (s, 1H, C*H*$_2$CCH$_3$, MMA), 3.47 (s, 9H, OCH$_3$, TMB), 3.44 (s, 3H, OCH$_3$, MMA), 3.42 (br s, 3H, OCH$_3$, PMMA), 1.91 (br s, 3H, CCH$_3$, PMMA), 1.77 (s, 3H, CH$_2$CC*H*$_3$, MMA), 1.04 (br s, 2H, CCH$_2$, PMMA).
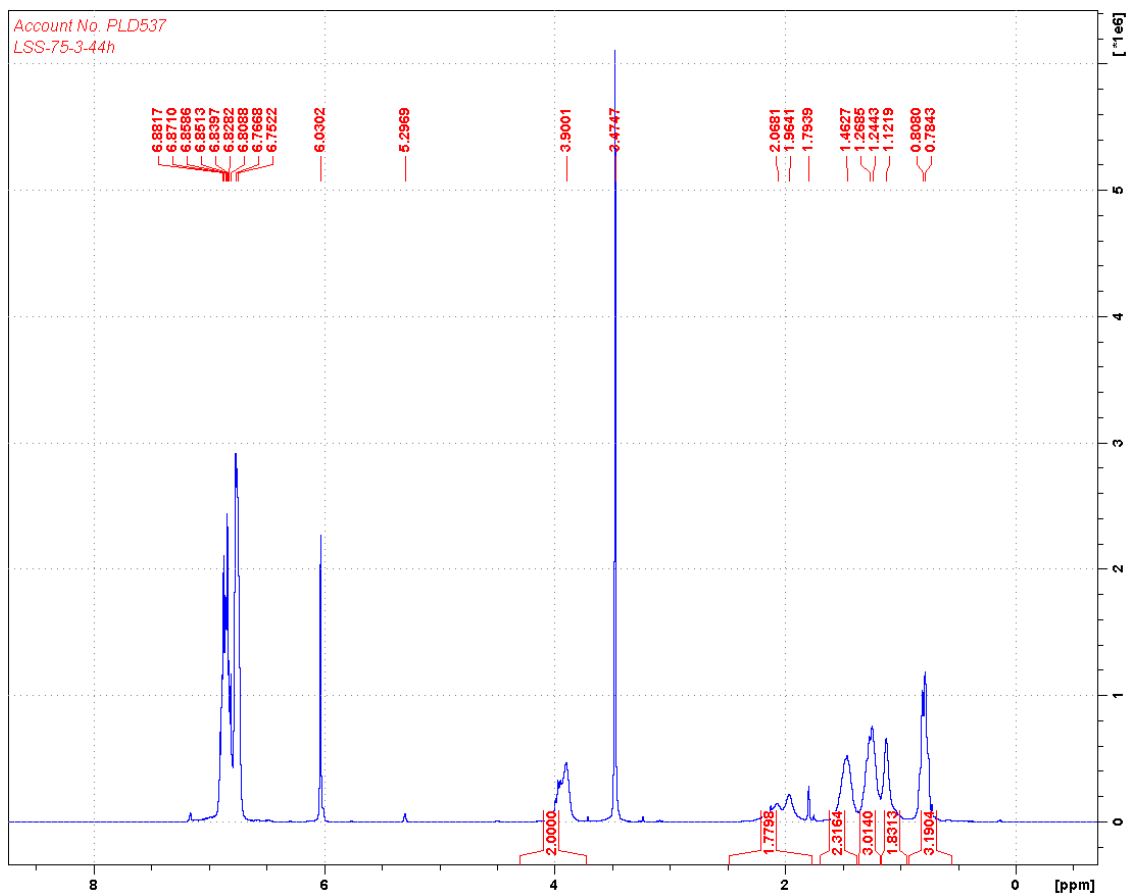
Figure S18. ^{1}H NMR (500 MHz, 25°C, C$_6$D$_6$) spectrum of 100 equivalents of *n*-BuMA polymerization by (fc^{P,B})NiBr (Table 1, entry 7). δ (ppm): 6.66-6.97 (m, 4H, 1,2-difluorobenzene), 6.03 (s, 3H, TMB), 5.29 (s, 1H, C*H*$_2$CCH$_3$, *n*-BuMA), 3.90 (br t, 2H, OC*H*$_2$CH$_2$CH$_2$CH$_3$, P*n*-BuMA), 3.47 (s, 9H, OCH$_3$, TMB), 1.96 (m, 2H, OCH$_2$C*H*$_2$CH$_2$CH$_3$, P*n*-BuMA), 1.46 (m, 2H, OCH$_2$CH$_2$C*H*$_2$CH$_3$, P*n*-BuMA), 1.24 (br s, 3H, CCH$_3$, P*n*-BuMA), 1.12 (br s, 2H, CCH$_2$, P*n*-BuMA), 0.78 (br t, 3H, CH$_2$C*H*$_3$, P*n*-BuMA).
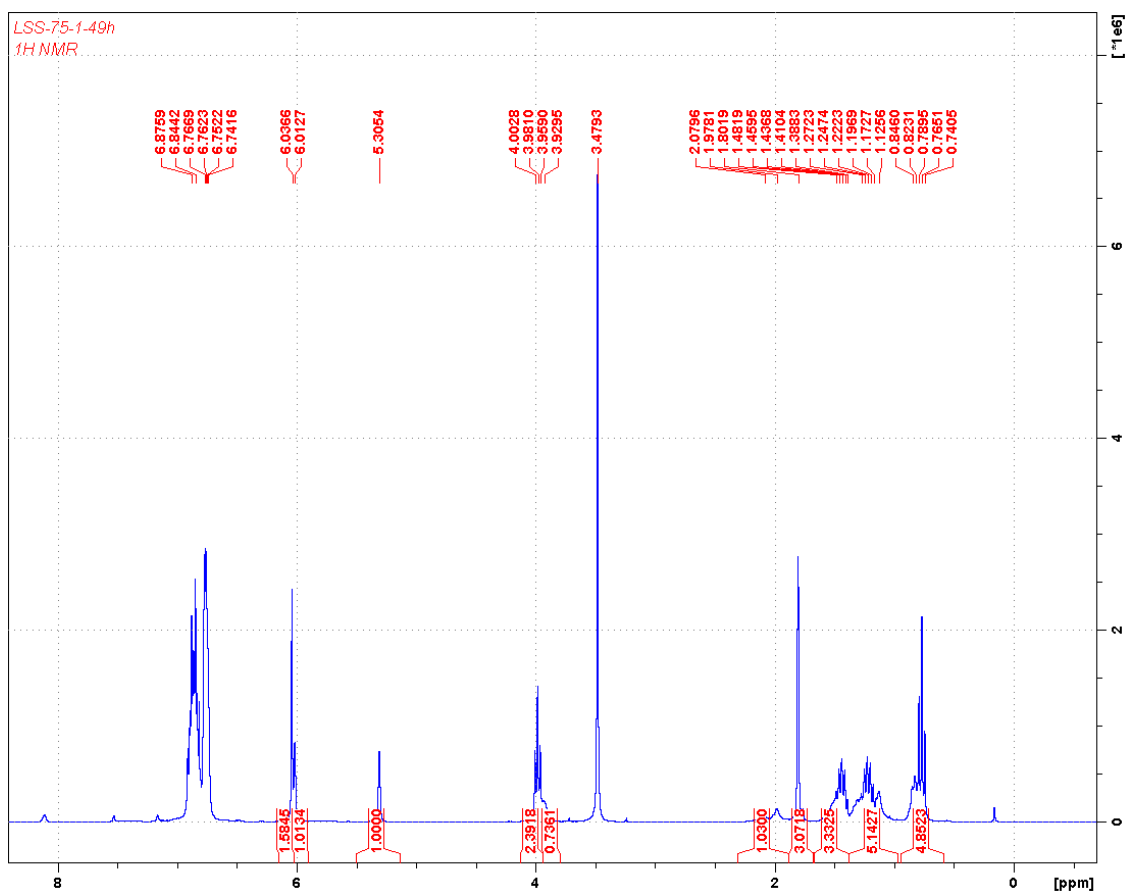
Figure S19. ^{1}H NMR (500 MHz, 25°C, C$_6$D$_6$) spectrum of 100 equivalents of *n*-BuMA polymerization by [(fc^{P,B})NiBr][BAr^F] (Table 1, entry 8). δ (ppm): 6.54-6.99 (m, 4H, 1,2-difluorobenzene), 6.04 (s, 3H, TMB), 6.01 (s, 1H, C*H*$_2$CCH$_3$, *n*-BuMA), 5.31 (s, 1H, C*H*$_2$CCH$_3$, *n*-BuMA), 3.96 (t, 2H, OC*H*$_2$CH$_2$, *n*-BuMA), 3.93 (br t, 2H, OC*H*$_2$CH$_2$, P*n*-BuMA), 3.48 (s, 9H, OCH$_3$, TMB), 1.98 (m, 2H, OCH$_2$C*H*$_2$CH$_2$CH$_3$, P*n*-BuMA), 1.80 (s, 3H, CCH$_3$, *n*-BuMA), 1.44 (m, 2H, OCH$_2$CH$_2$C*H*$_2$CH$_3$, P*n*-BuMA), 1.22 (m, 2H, OCH$_2$CH$_2$C*H*$_2$CH$_3$, *n*-BuMA), 1.13 (br s, 2H, CCH$_2$, P*n*-BuMA), 0.77 (br t, 3H, CH$_2$C*H*$_3$, *n*-BuMA and P*n*-BuMA).
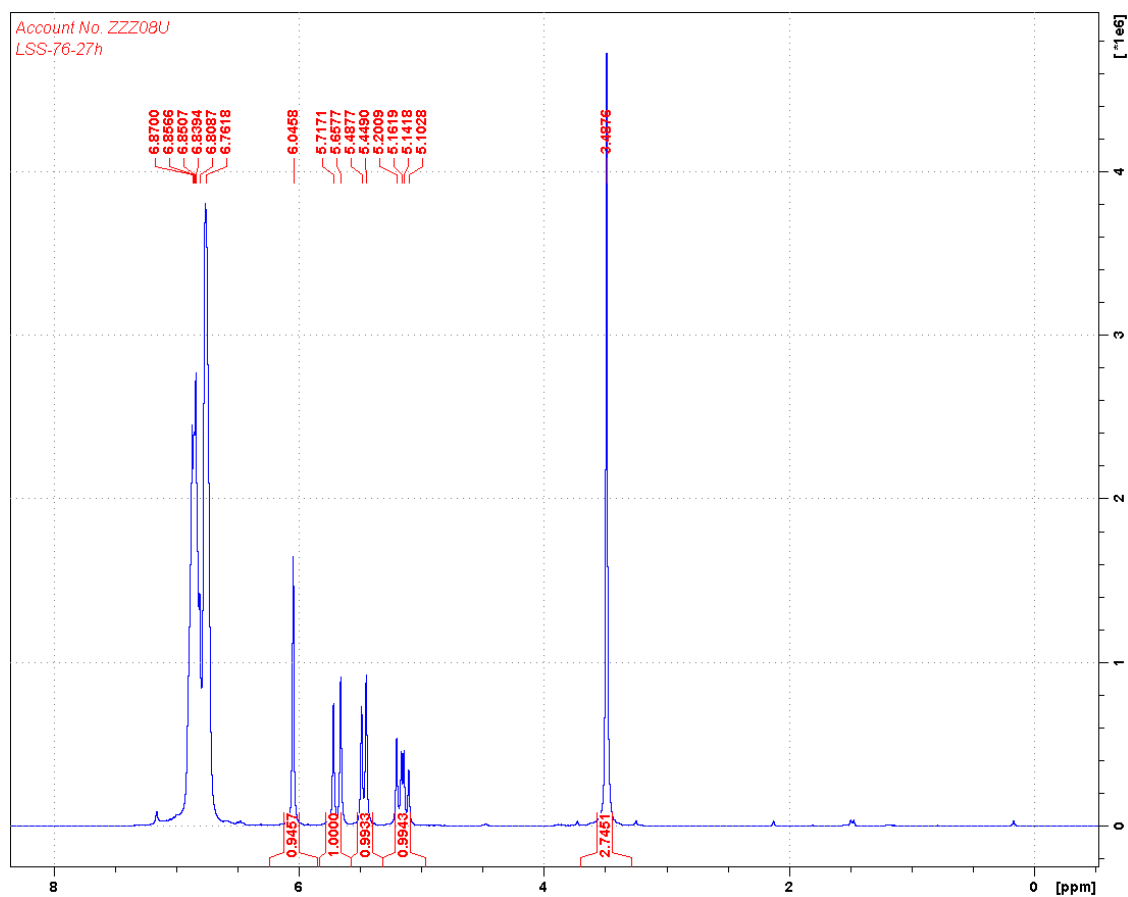
Figure S20. ^{1}H NMR (500 MHz, 25°C, C$_6$D$_6$) spectrum of 100 equivalents of acrylonitrile polymerization by (fc^{P,B})NiBr (Table 1, entry 9). δ (ppm): 6.54-7.05 (m, 4H, 1,2-difluorobenzene), 6.05 (s, 3H, TMB), 5.66 (dd, 1H, C*H*$_2$CHC, acrylonitrile), 5.45 (dd, 1H, C*H*$_2$CHC, acrylonitrile), 5.10 (dd, 1H, CH$_2$C*H*C, acrylonitrile), 3.49 (s, 9H, OCH$_3$, TMB).
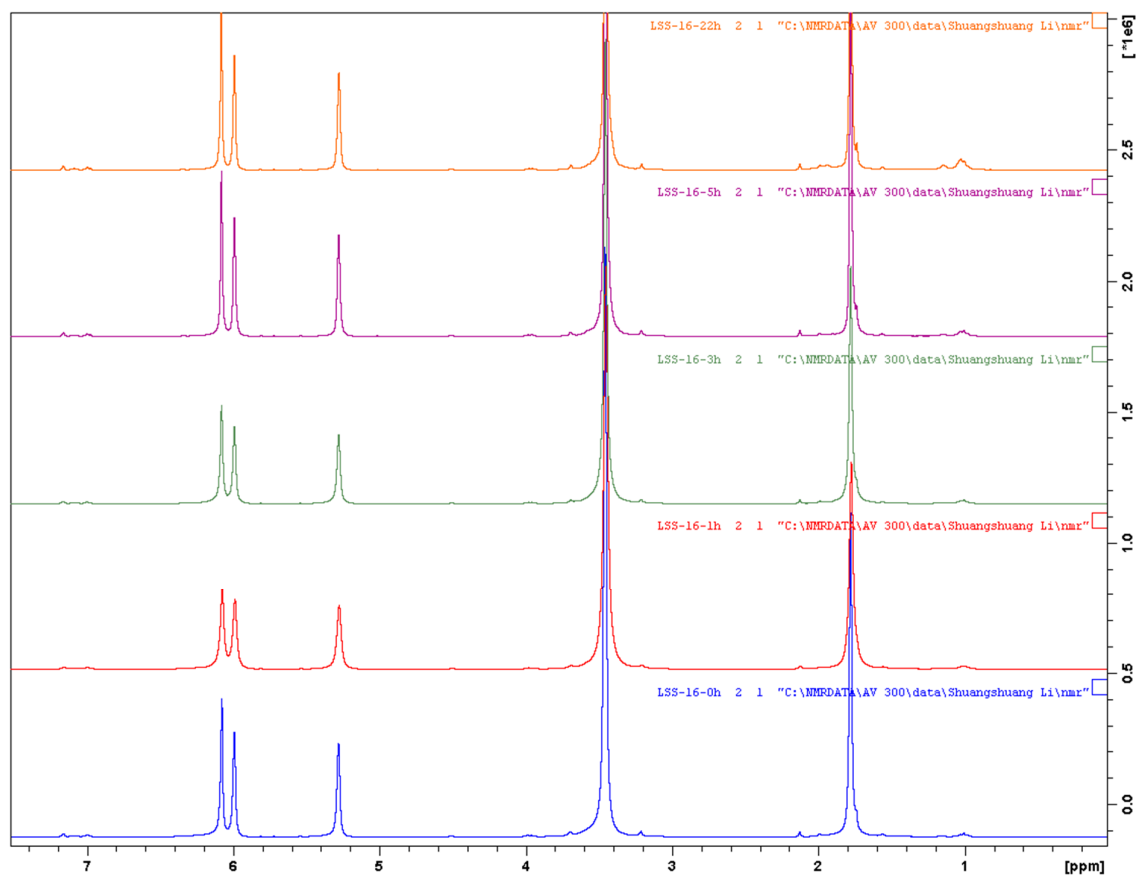
Figure S21. ^{1}H NMR (500 MHz, 25°C, C_6D_6) spectra of 95 equivalents of MMA polymerization by (fc[P,B])NiBr (Table S1, entry 15) at ambient temperature at (from top to bottom): 0, 1, 3, 5, 22 h.
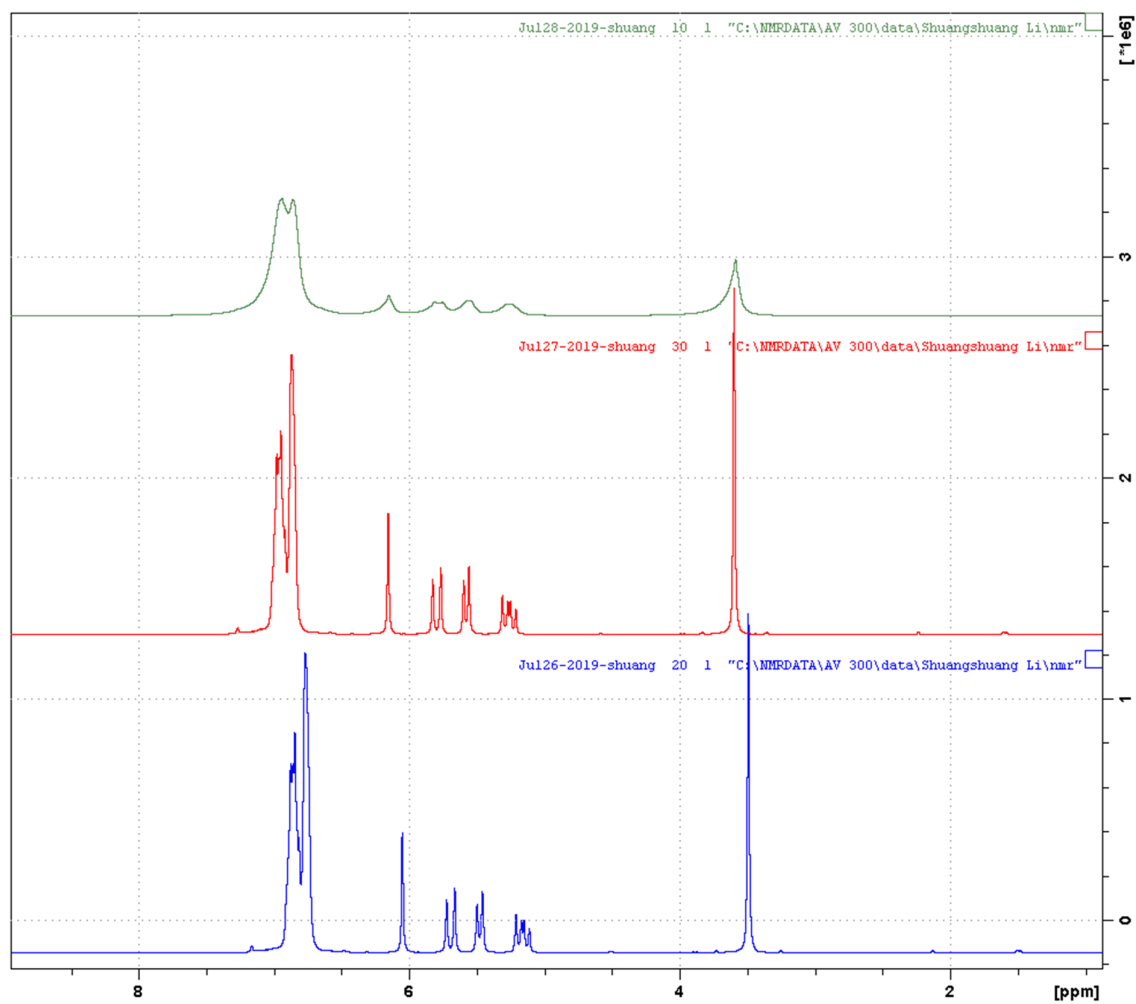
Figure S22. ^{1}H NMR (500 MHz, 25°C, C$_6$D$_6$) spectrum of 100 equivalents of acrylonitrile polymerization by (fc^{P,B})NiBr (Table S1, entry 16) after (from top to bottom): 24 h at ambient temperature, an additional 4 h at 60 ℃, and another 50 h at 80 ℃.
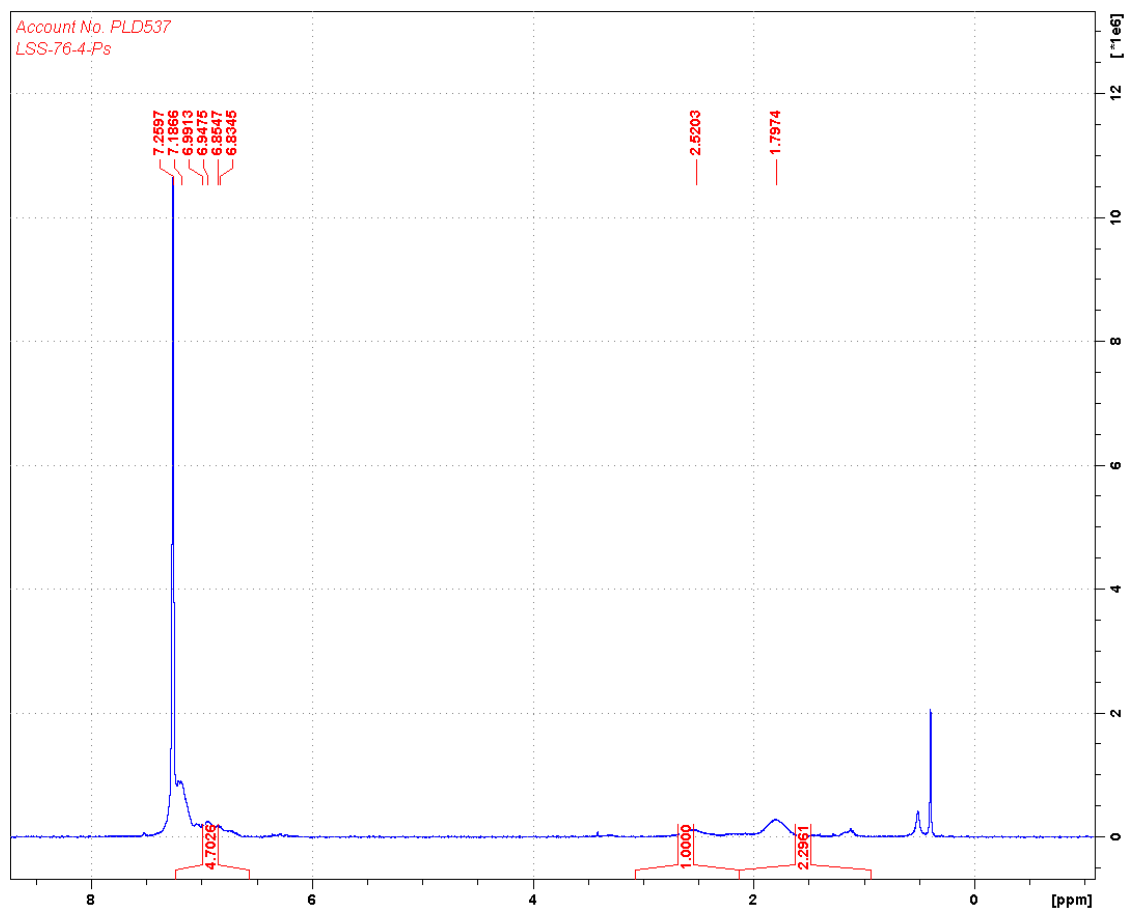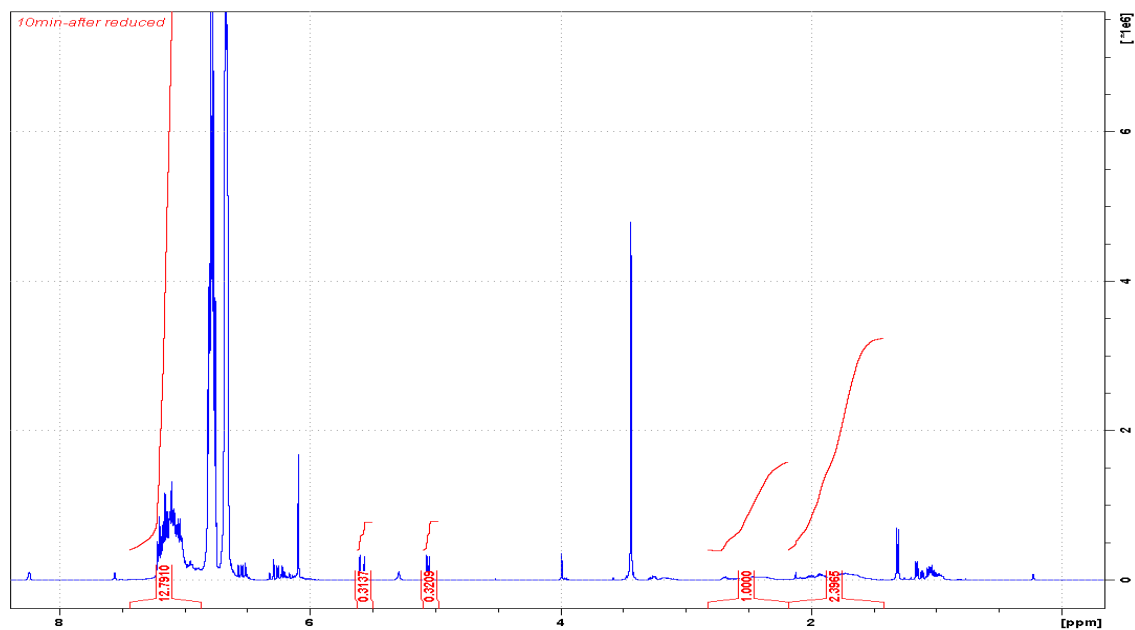
Figure S23. ^{1}H NMR (300 MHz, 25°C) spectra of PS polymerization reaction in C_6D_6 (top) and the isolated polymer of PS in $CDCl_3$ (bottom, Table 2, entry 1). δ (ppm): 7.19 (m, 5H, ArH, PS), 2.52 (br t, 1H, C*H*CH$_2$, PS), 1.79 (br d, 2H, CHC*H*$_2$, PS).
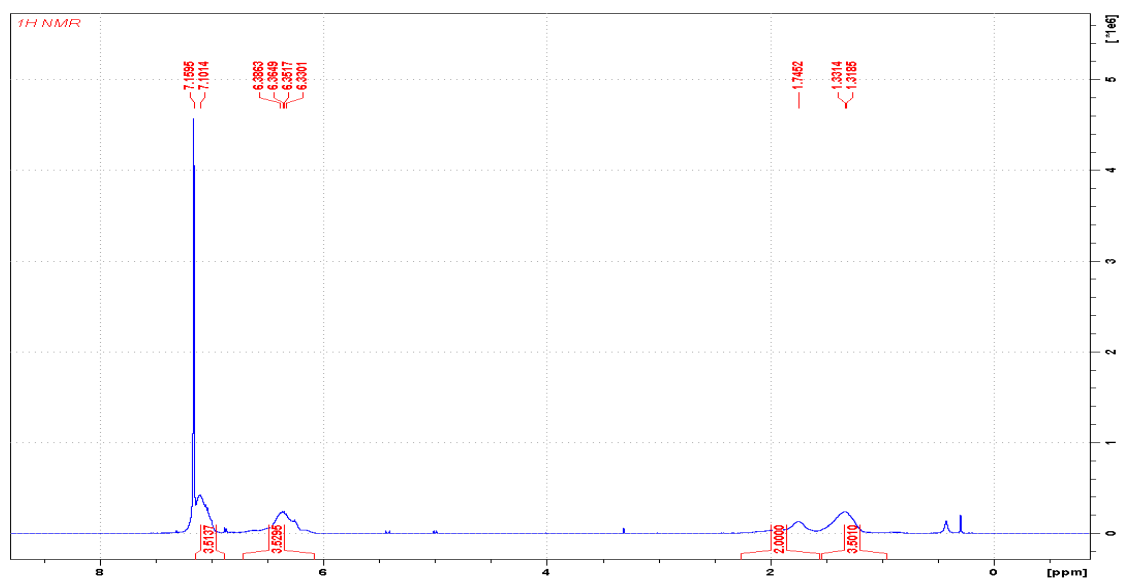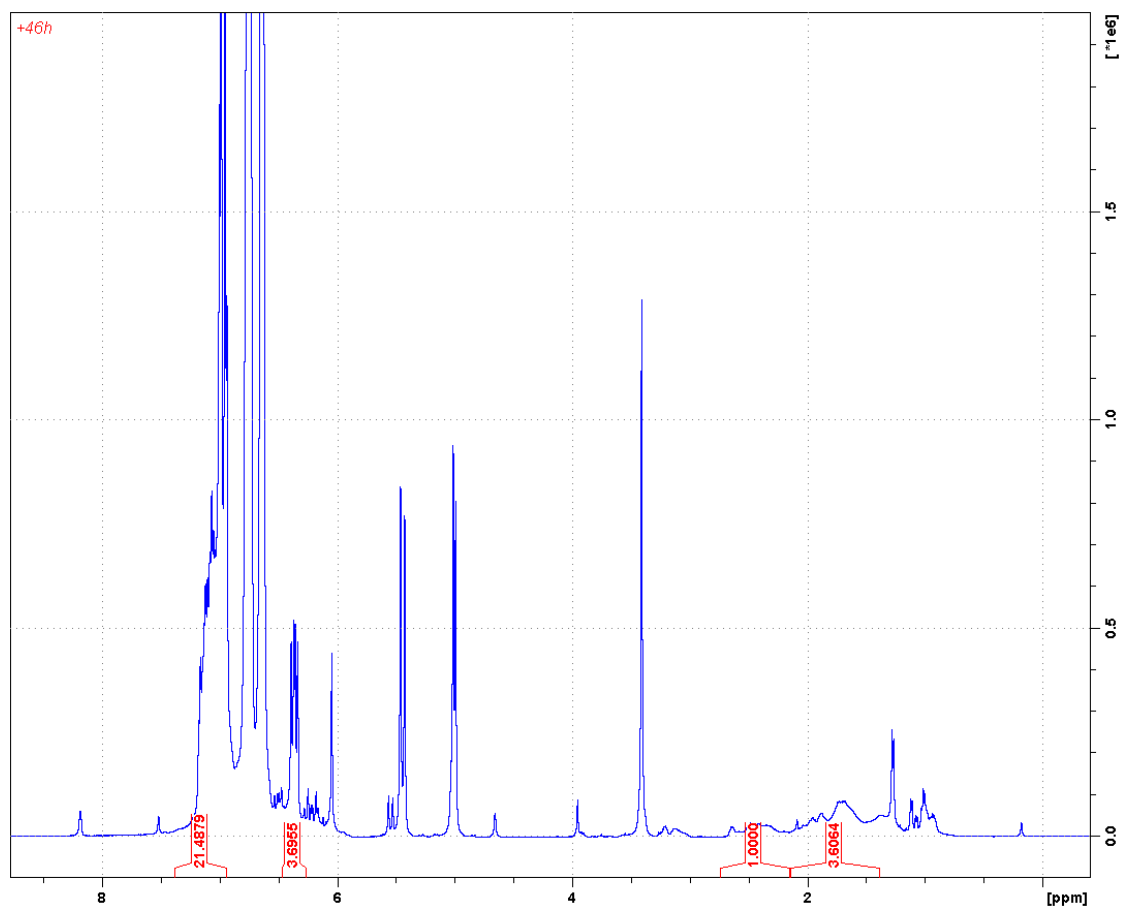
Figure S24. ^{1}H NMR (500 MHz, 25°C) spectra of PS-PCS copolymerization reaction after adding p-CS sequentially in C$_6$D$_6$ (top) and the isolated copolymer of PS-PCS in C$_6$D$_6$ (bottom, Table 2, entry 2). δ (ppm): 7.10 (m, 2H, ArH, PS and PCS), 6.33 (m, 2H, ArH, PCS), 1.75 (br t, 1H, C*H*CH$_2$, PS and PCS), 1.32 (br d, 2H, CHC*H*$_2$, PS and PCS).
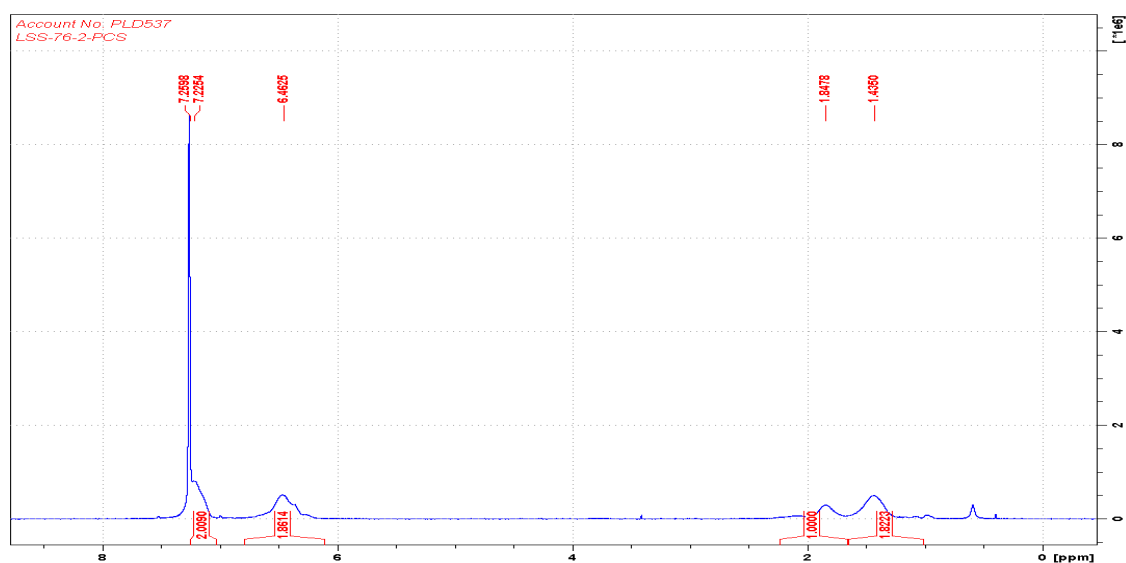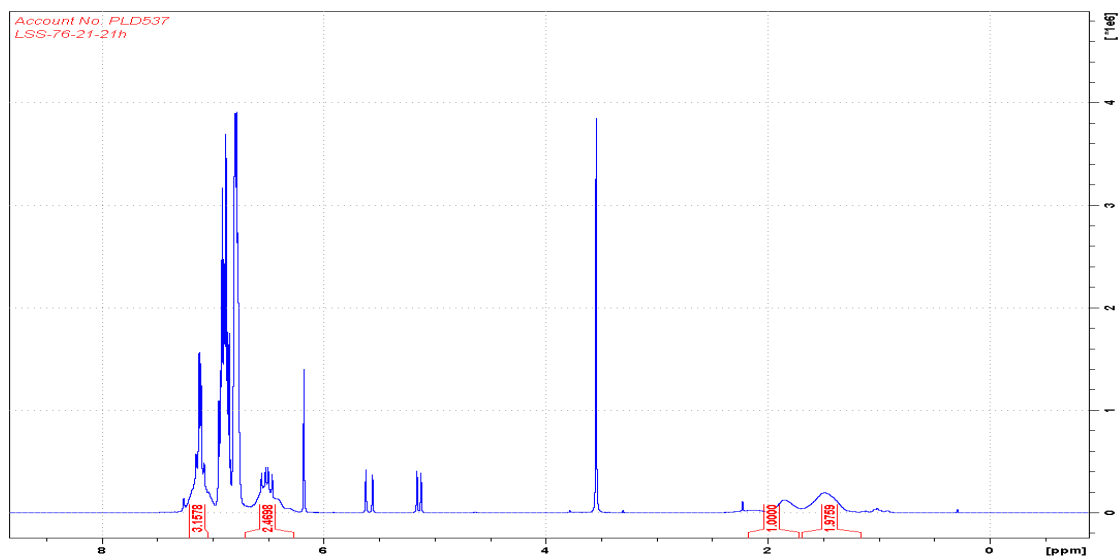
Figure S25. ^{1}H NMR (300 MHz, 25°C) spectra of *p*-CS polymerization reaction in C$_6$D$_6$ (top) and the isolated polymer of PCS in CDCl$_3$ (bottom, Table 2, entry 3). δ (ppm): 7.22 (m, 2H, ArH, PCS), 6.46 (m, 2H, ArH, PCS), 1.85 (br t, 1H, C*H*CH$_2$, PCS), 1.43 (br d, 2H, CHC*H*$_2$, PCS).
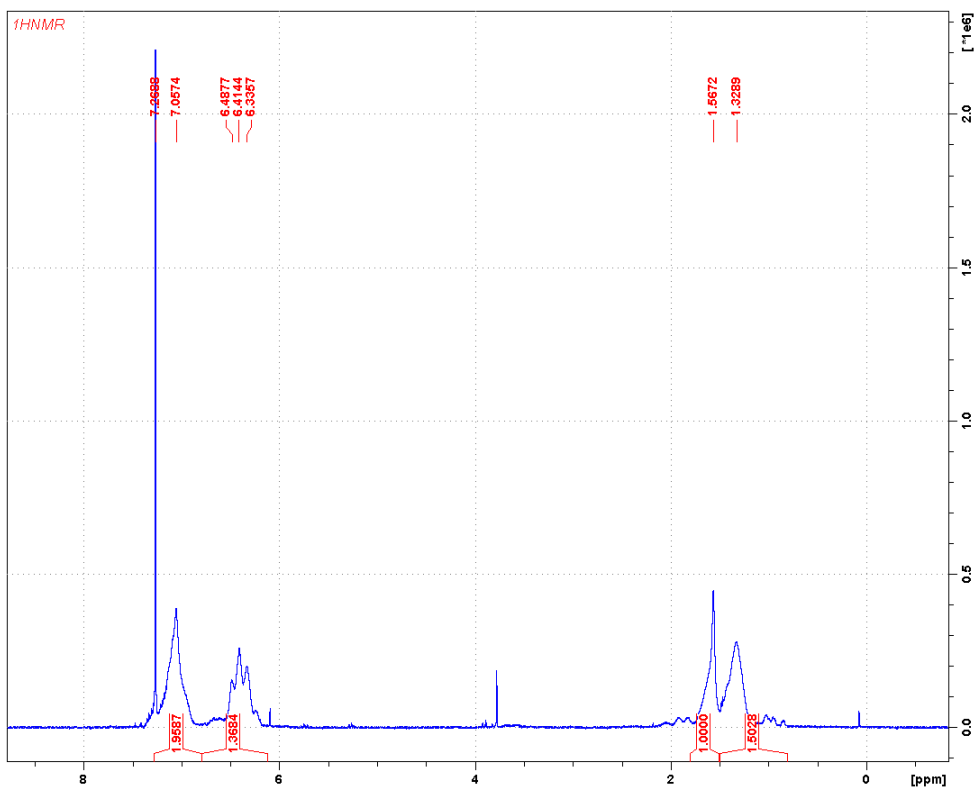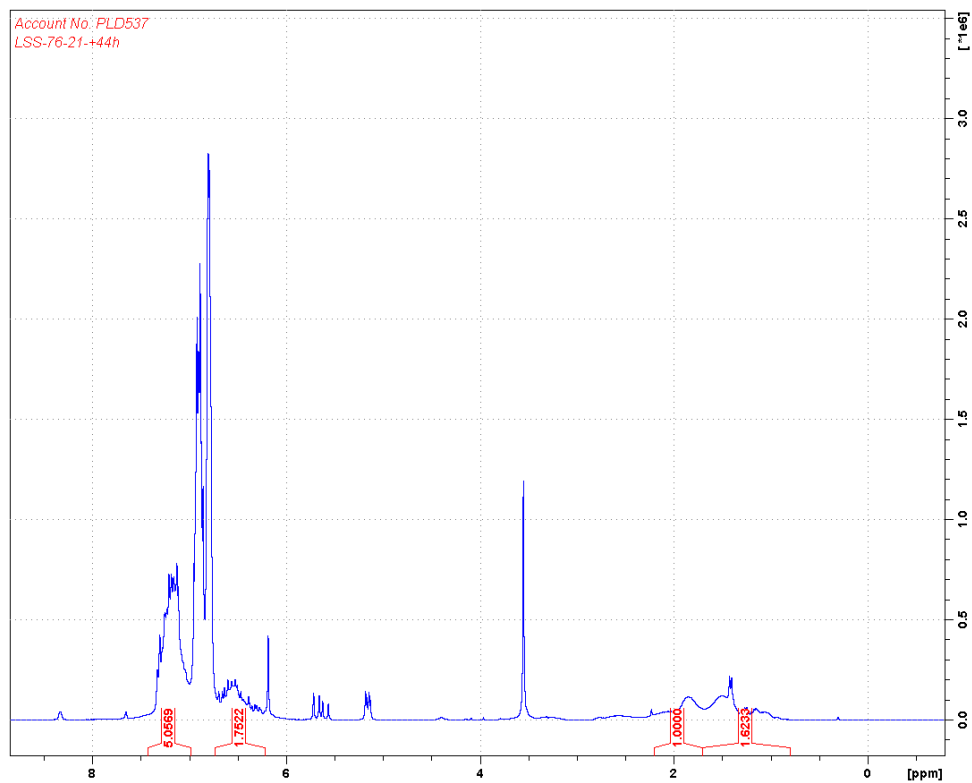
Figure S26. ^{1}H NMR (300 MHz, 25°C) spectra of PCS-PS copolymerization reaction in C_6D_6 (top) after adding styrene sequentially and the isolated polymer of PCS-PS in CDCl$_3$ (bottom, Table 2, entry 4). δ (ppm): 7.06 (m, 2H, ArH, PS and PCS), 6.33 (m, 2H, ArH, PCS), 1.57 (br t, 1H, C*H*CH$_2$, PS and PCS), 1.33 (br d, 2H, CHC*H*$_2$, PS and PCS).
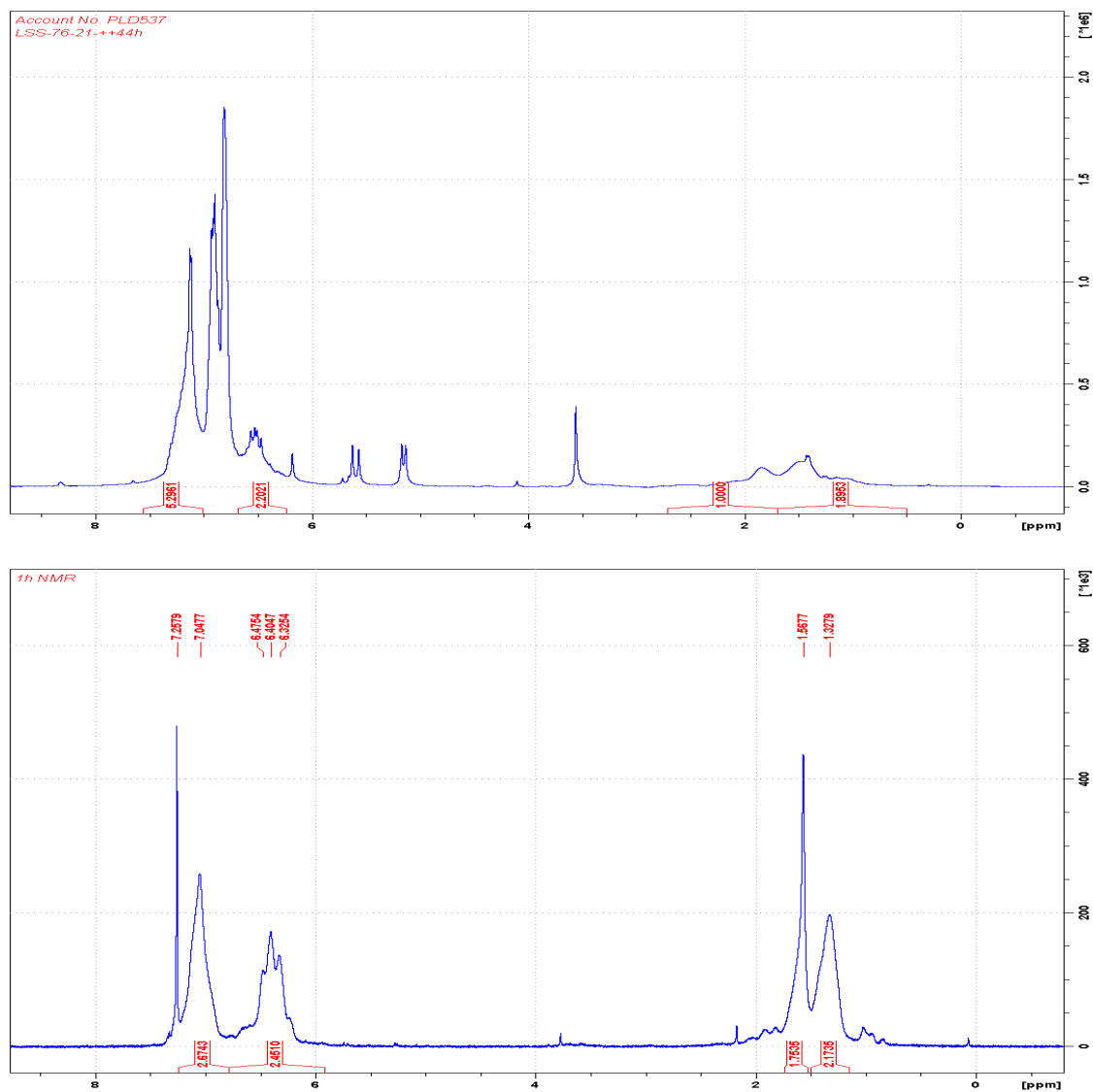
23

Figure S27. ^{1}H NMR (300 MHz, 25°C) spectra of PCS-PS-PCS copolymerization reaction after adding p-CS again in C$_6$D$_6$ (top) and the isolated polymer of PCS-PS-PCS in CDCl$_3$ (bottom, Table 2, entry 5). δ (ppm): 7.05 (m, 2H, ArH, PS and PCS), 6.33 (m, 2H, ArH, PCS), 1.57 (br t, 1H, C*H*CH$_2$, PS and PCS), 1.33 (br d, 2H, CHC*H*$_2$, PS and PCS).
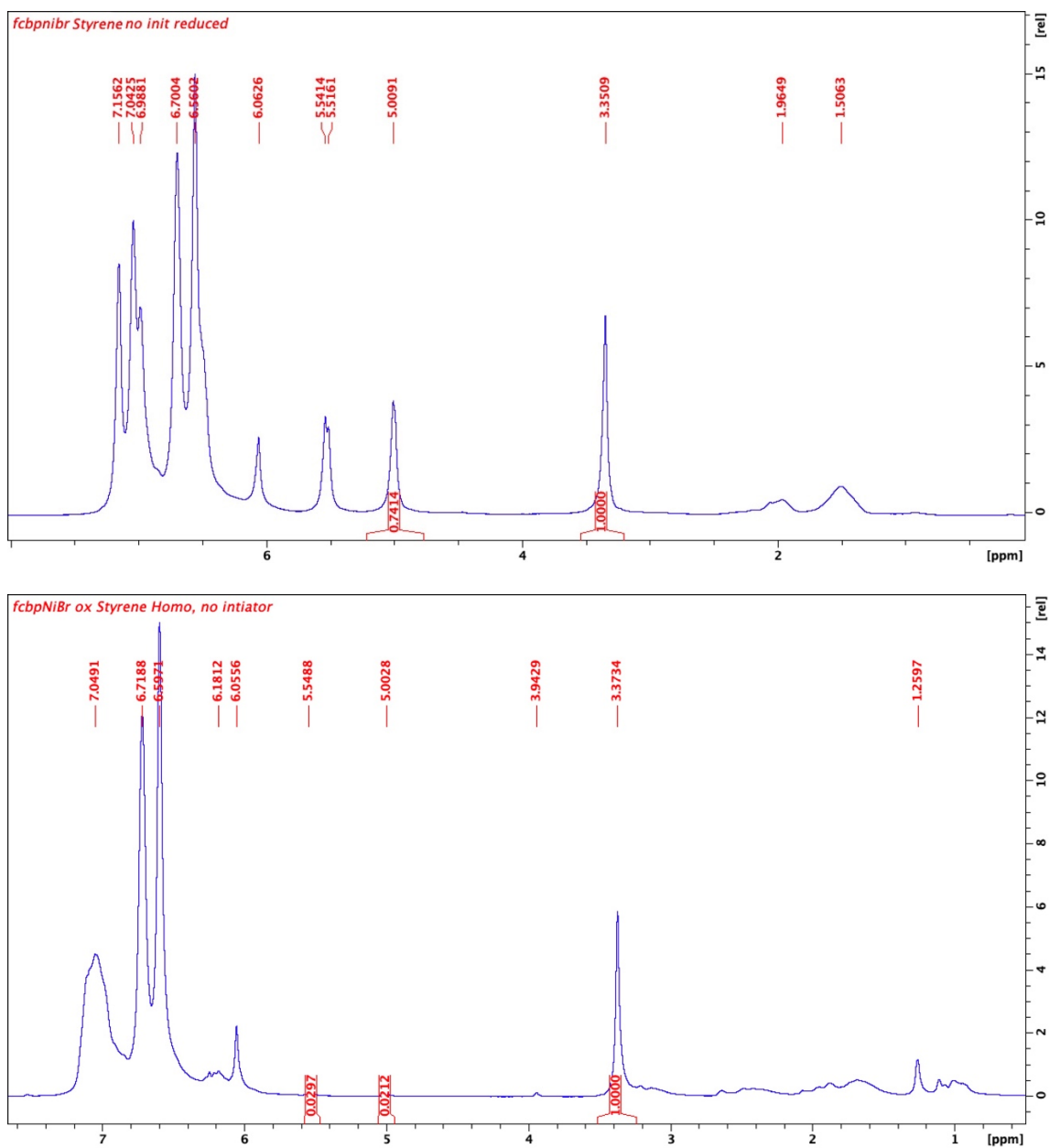
Figure S28. ^{1}H NMR (600 MHz, 25°C, C$_6$D$_6$) spectra of 100 equivalents of styrene polymerization by (fc^{P,B})NiBr (top) and [(fc^{P,B})NiBr][BAr^F] (bottom) in the absence of a radical initiator (Table S1, entries 1 & 2). δ (ppm): 7.02 (m, 5H, ArH, PS), 6.46-6.85 (m, 4H, 1,2-difluorobenzene), 6.04 (s, 3H, TMB), 3.41 (s, 9H, OCH$_3$, TMB), 2.45 (br t, 1H, C*H*CH$_2$, PS), 1.88 (br d, 2H, CHC*H$_2$*, PS).
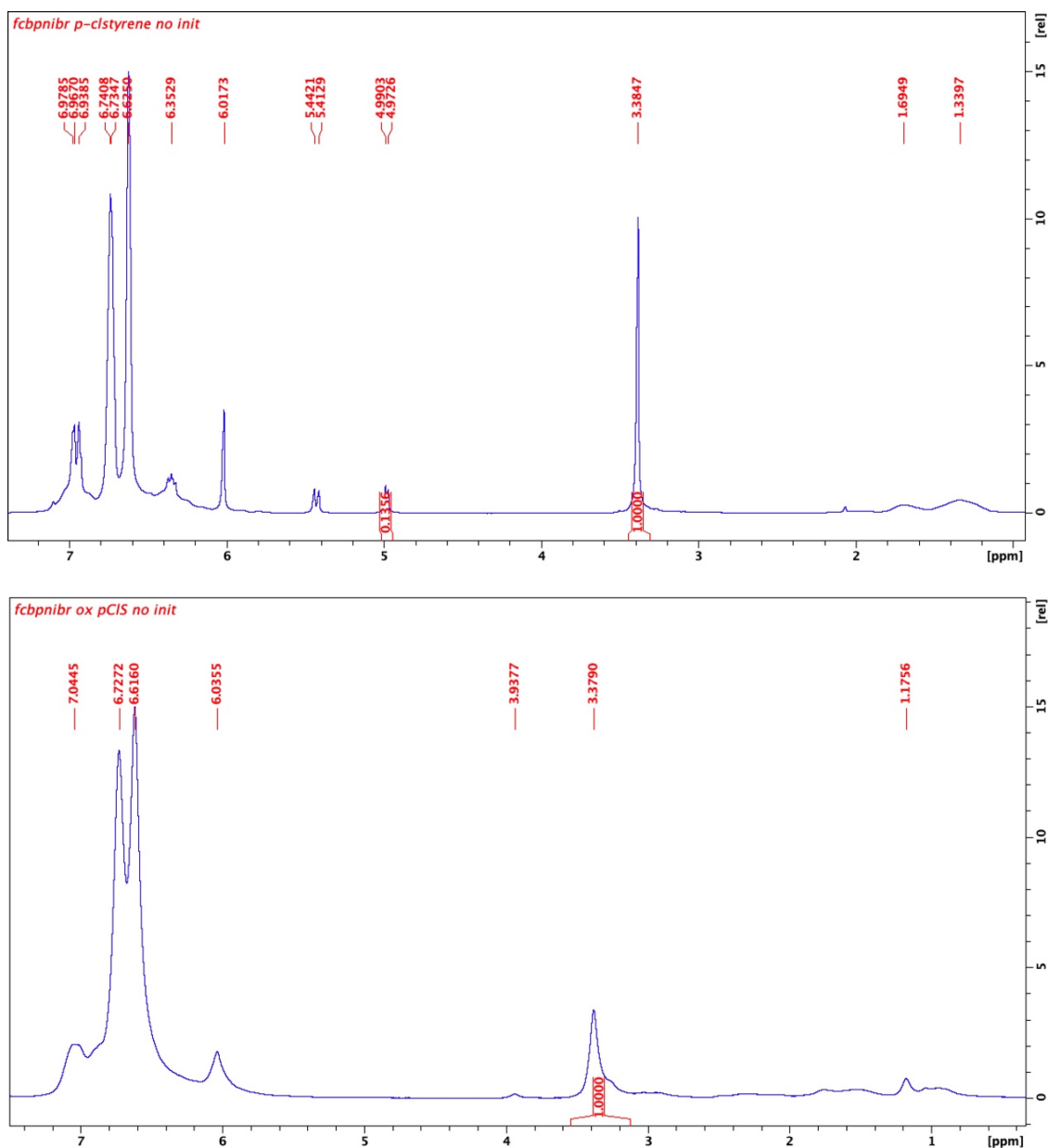
Figure S29. ^{1}H NMR (600 MHz, 25°C, C_6D_6) spectra of 100 equivalents of *p*-chlorostyrene polymerization by (fc^{P,B})NiBr (top) and [(fc^{P,B})NiBr][BAr^F] (bottom) in the absence of a radical initiator (Table S1, entries 3 & 4). δ (ppm): 7.02 (m, 2H, ArH, PCS), 6.58-6.89 (m, 4H, 1,2-difluorobenzene), 6.42 (m, 2H, ArH, PCS), 6.07 (s, 3H, TMB), 5.50 (br dd, 1H, CHC*H₂*, p-CS), 5.05 (br dd, 1H, CHC*H₂*, p-CS), 3.44 (s, 9H, OCH₃, TMB), 1.75 (br t, 1H, C*H*CH₂, PCS), 1.38 (br d, 2H, CHC*H₂*, PCS).

26

SEC data
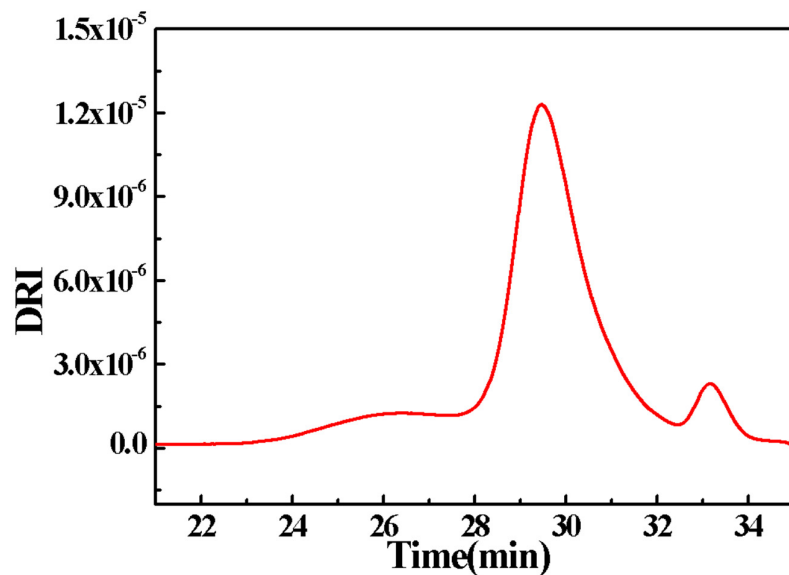
Figure S30. SEC trace for polymerization of 100 equivalents of styrene using [(fc^{P,B})NiBr][BAr^F] at 25 °C (Table 1, entry 2).
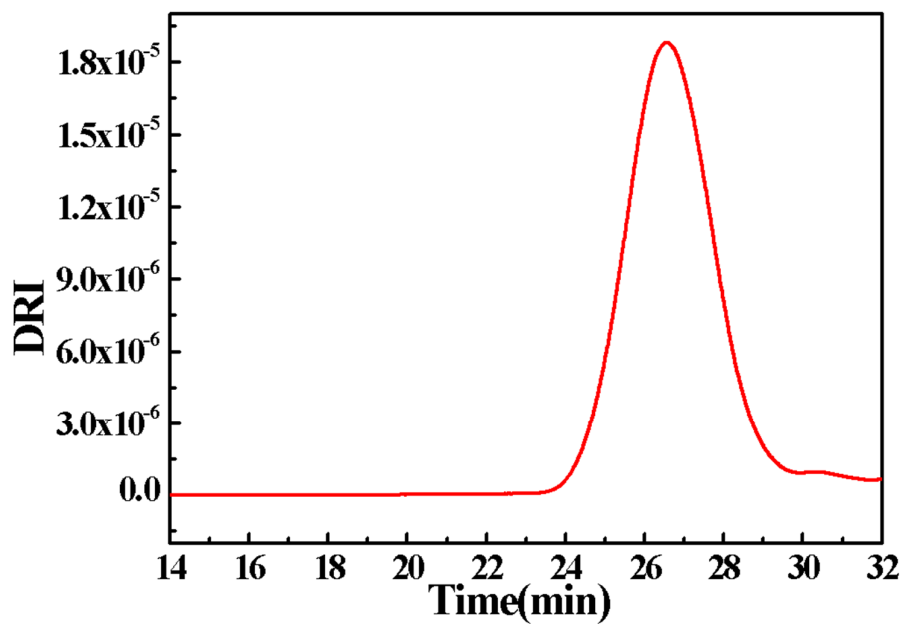
Figure S31. SEC trace for polymerization of 100 equivalents of *p*-CS using (fc^{P,B})NiBr at 80 °C (Table 1, entry 3).
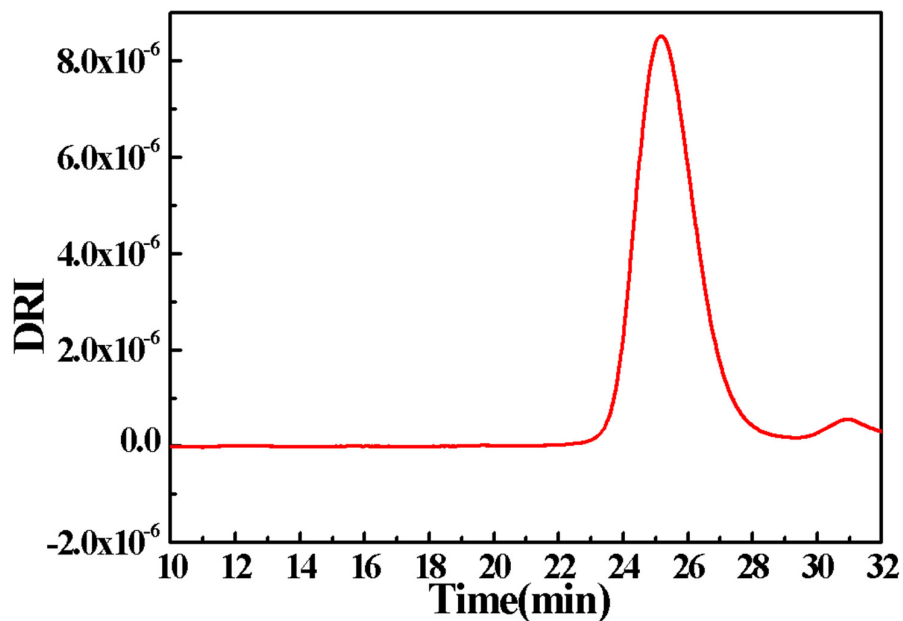
Figure S32. SEC trace for polymerization of 100 equivalents of MMA using [(fc^{P,B})NiBr][BAr^F] at 25 °C (Table 1, entry 6).
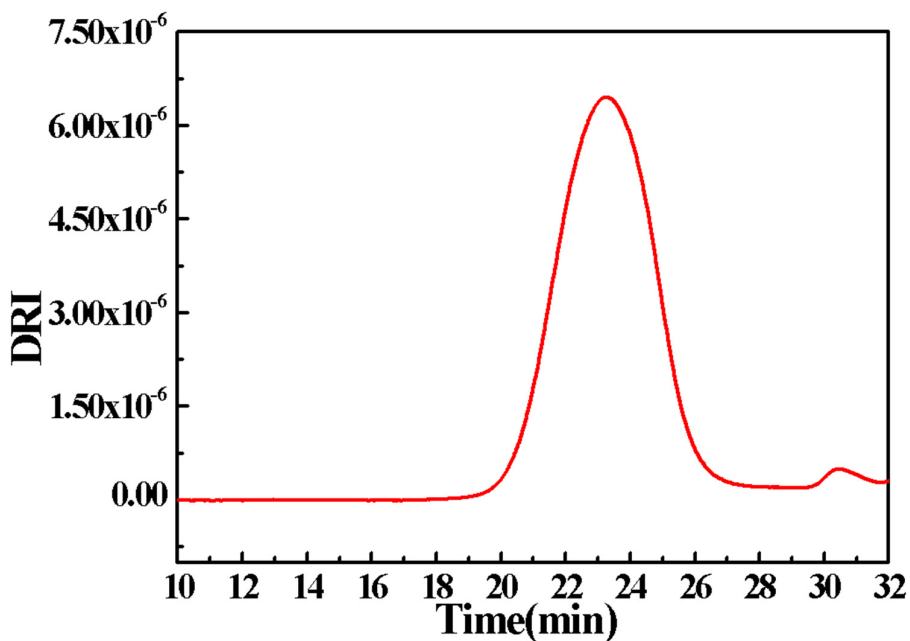
Figure S33. SEC trace for polymerization of 100 equivalents of *n*-BuMA using (fc^{P,B})NiBr at 80 °C (Table 1, entry 7).
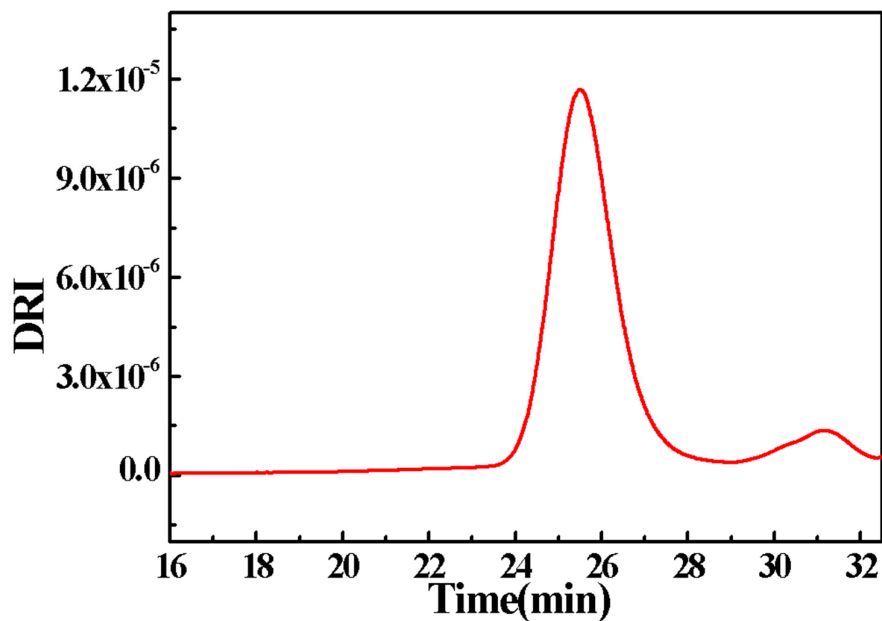
Figure S34. SEC trace for polymerization of 100 equivalents of *n*-BuMA using [(fc^{P,B})NiBr][BAr^F] at 25 °C (Table 1, entry 8).
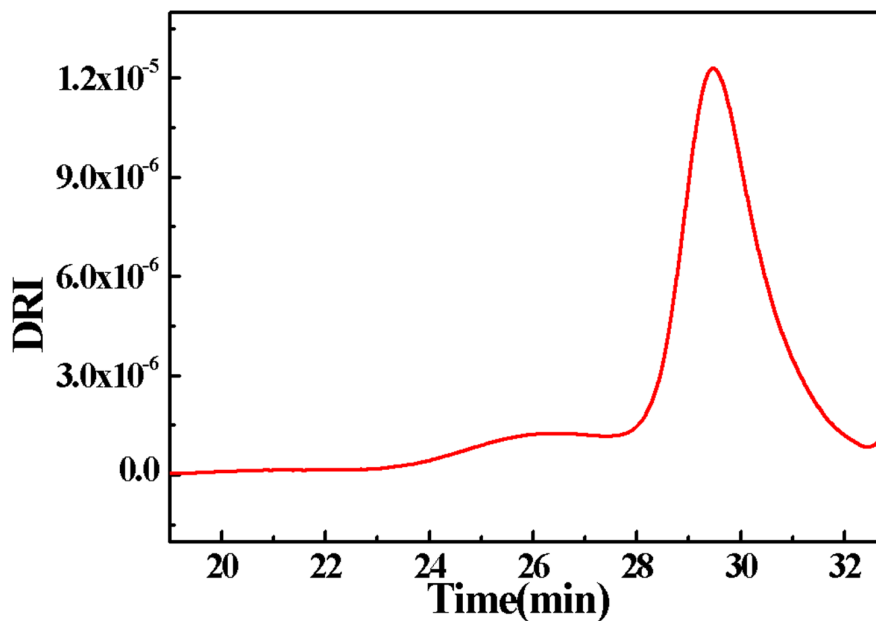
Figure S35. SEC trace of PS homopolymer using [(fc^{P,B})NiBr][BAr^F] at 25 °C (Table 2, entry 1).
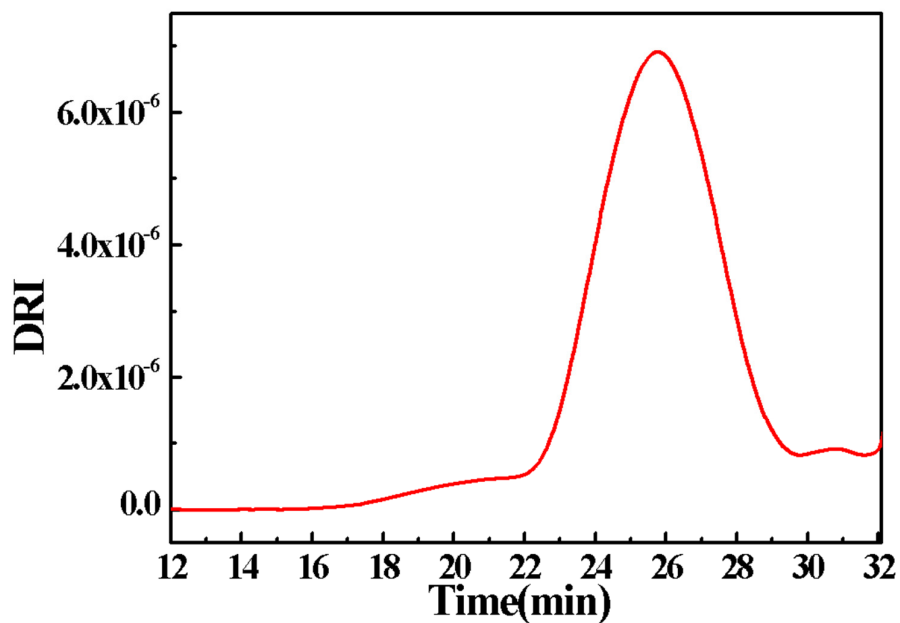
Figure S36. SEC trace of PS-PCS di-block copolymer using (fc^{P,B})NiBr and [(fc^{P,B})NiBr][BAr^F] (Table 2, entry 2).
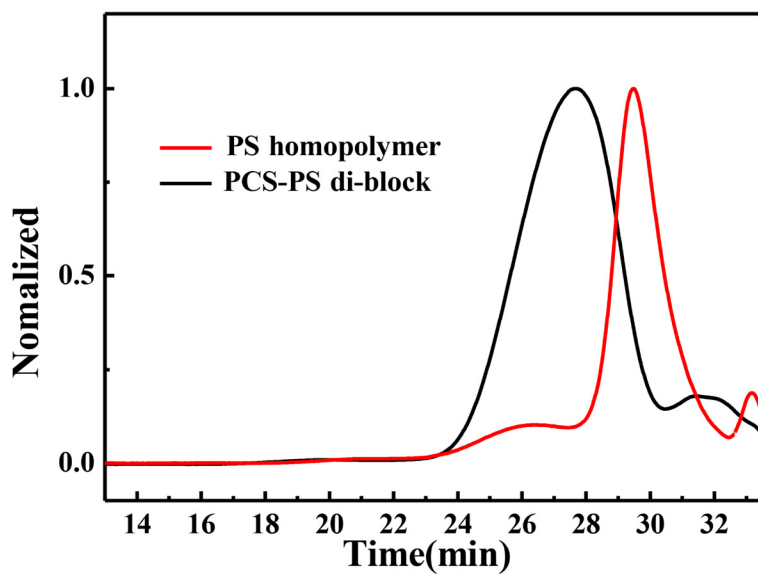
Figure S37. SEC trace of the PS-PCS diblock copolymer and PS homopolymer (Table 2, entries 1 and 2).
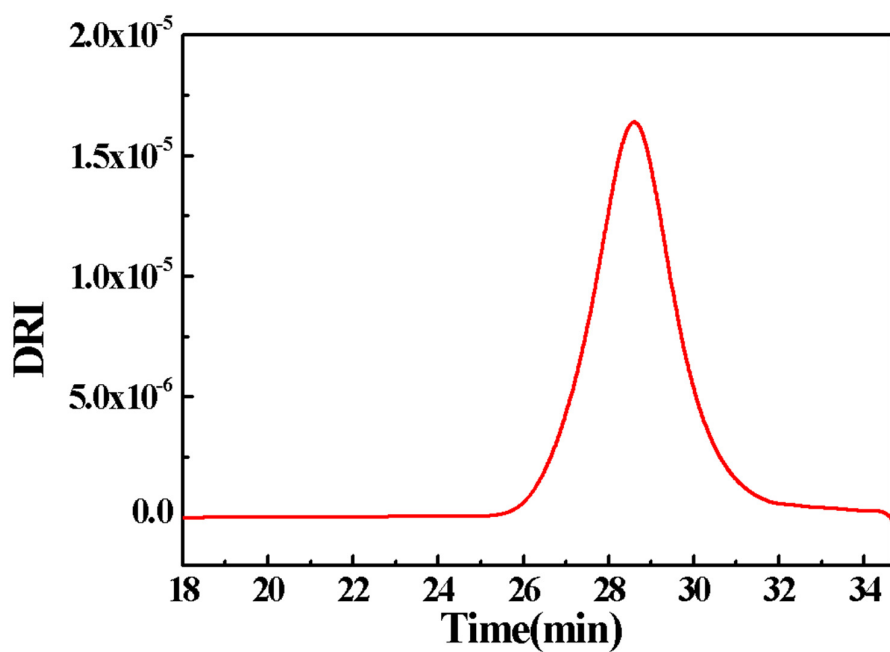
Figure S38. SEC trace of PCS homopolymer using $(fc^{P,B})NiBr$ at 25°C (Table 2, entry 3).
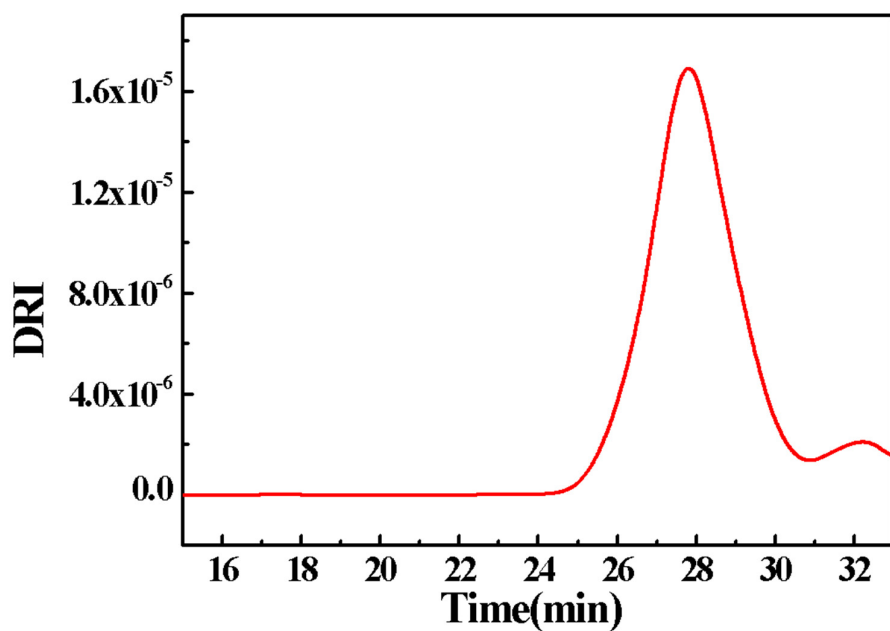
Figure S39. SEC trace of PCS-PS di-block copolymer using $(fc^{P,B})NiBr$ and $[(fc^{P,B})NiBr][BAr^F]$ (Table 2, entry 4).
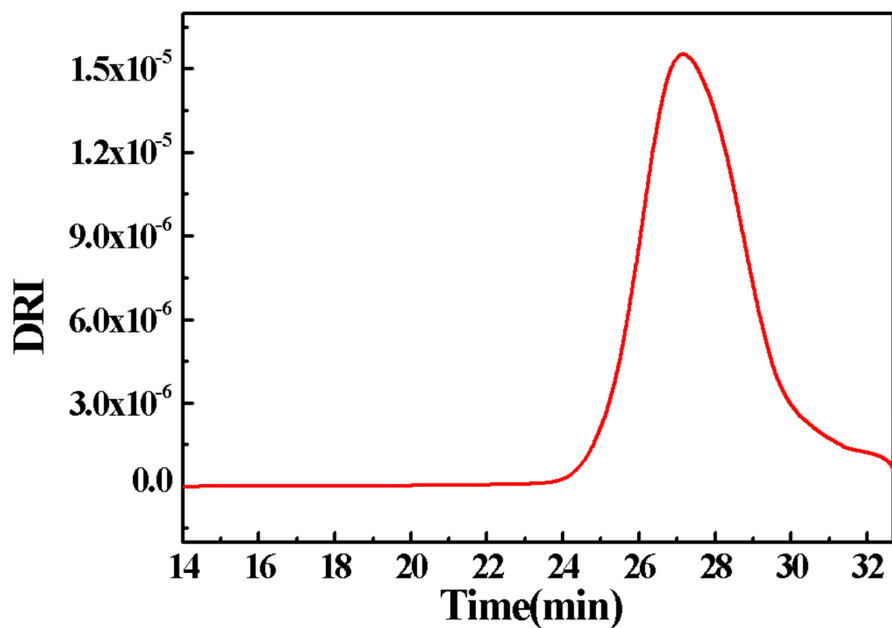
Figure S40. SEC trace of PCS-PS-PCS tri-block copolymer using (fc^{P,B})NiBr and [(fc^{P,B})NiBr][BAr^F] (Table 2, entry 5).
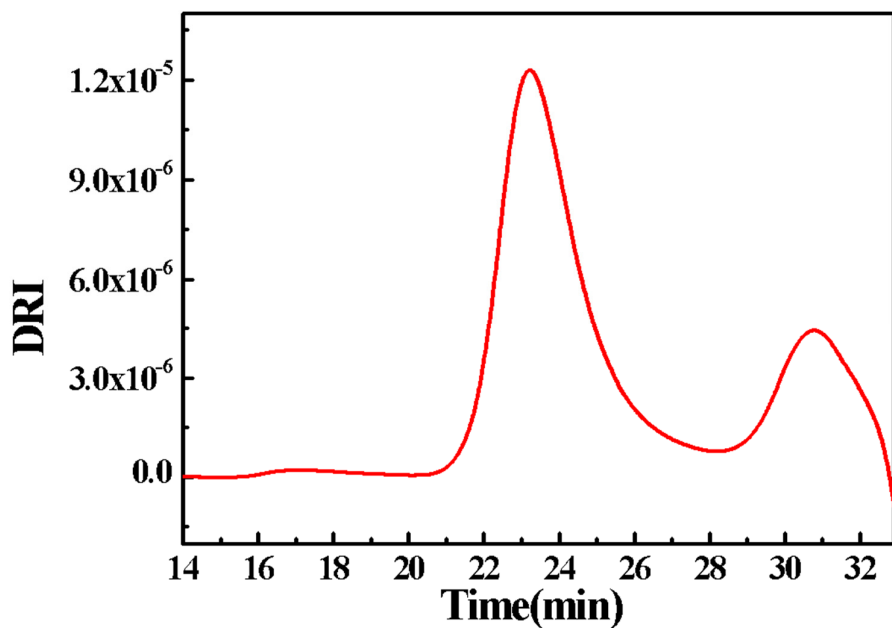
Figure S41. SEC trace of PS-PCS-PS tri-block copolymer using (fc^{P,B})NiBr and [(fc^{P,B})NiBr][BAr^F] (Table S2, entry 5).
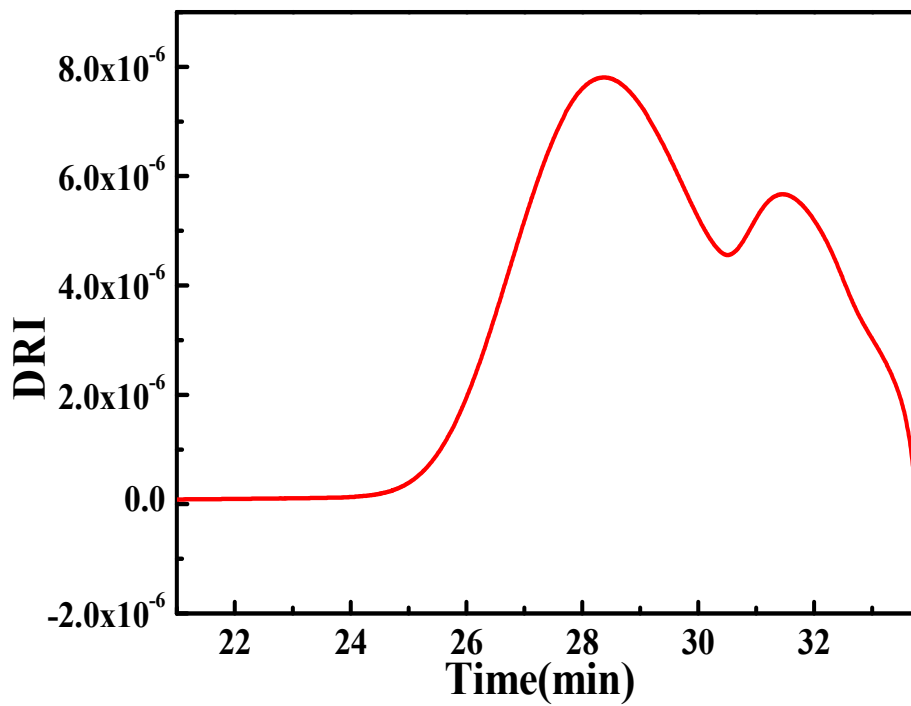
Figure S42. SEC trace of PS-PCS polymer obtain using a one pot synthesis by (fc^{P,B})NiBr and [(fc^{P,B})NiBr][BAr^F].

EPR experiments

The samples were prepared in 2-MeTHF (1 mM) and were frozen in 3 mm outer diameter quartz tubes inside a nitrogen-filled glovebox. The tubes were then sealed with a plastic cap and electrical tape and taken to the spectrometer. The samples were submerged in a liquid nitrogen-filled finger Dewar and X-band continues wave EPR spectra were obtained using Bruker EMX spectrometer. Given that the reduced compound has a spin = 1 because of the tetrahedral Ni(II) compound, no signal could be observed at 77 K. Furthermore, the oxidized compound also did not show any signals.
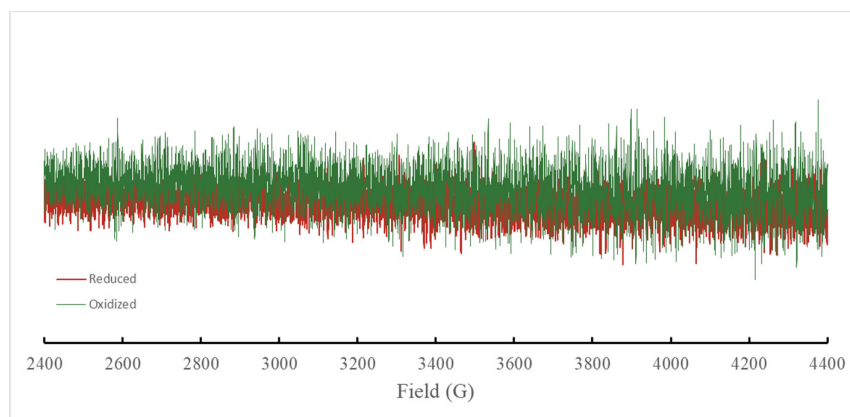
Figure S43. EPR spectra of the oxidized and reduced Ni compounds at 77 K.

Molar absorptivity study
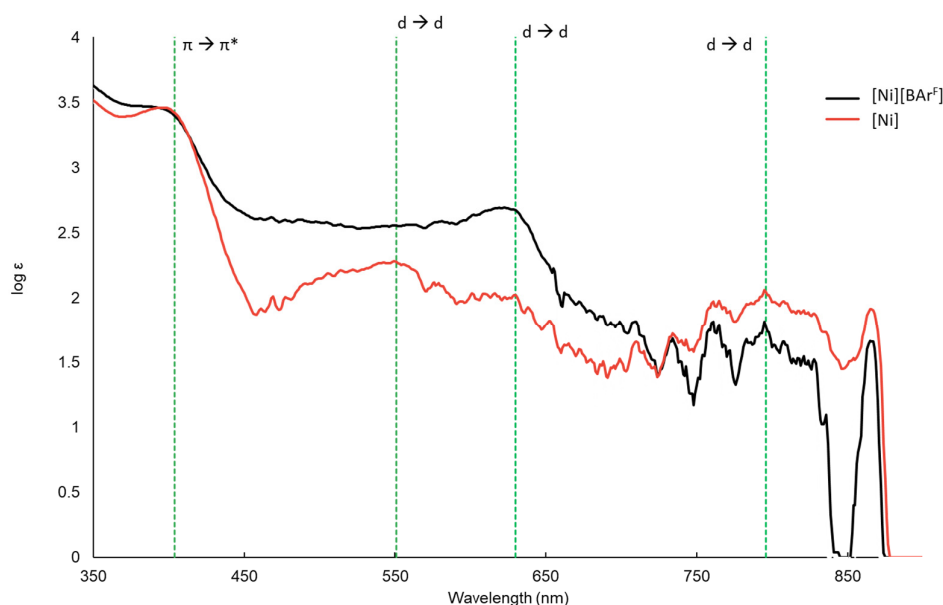
Figure S44. Plot of log (molar absoroptivity) vs. wavelength of (fc^{P,B})NiBr (abbreviated to [Ni]) and [(fc^{P,B})NiBr][BAr^F] (abbreviated to [Ni][BAr^F]). Both spectra were collected in 1,2-difluorobenzene at 0.29 mM concentration.

ICP-MS study

The concentrations of iron and nickel in $[(fc^{P,B})NiBr][BAr^F]$ were measured by an Agilent QQQ ICP-MS (Agilent Technologies) instrument. The compound was stirred overnight in 1 mL of concentrated nitric acid before dilution to form a 2% nitric acid solution in water. Two successive 25-fold dilutions of this solution with 2% nitric acid were then performed. Scandium was used as an internal standard (IS) during measurement. Isotopes ^{56}Fe, ^{60}Ni, and ^{45}Sc (IS) were measured for all samples. A set of calibration standards (0, 1, 10, 50, 100, 200, 500 ng/mL of Fe and Ni) was used for quantification. H_2 was used as a reactor gas for ^{56}Fe and He as a collision gas for ^{60}Ni and ^{45}Sc measurements.
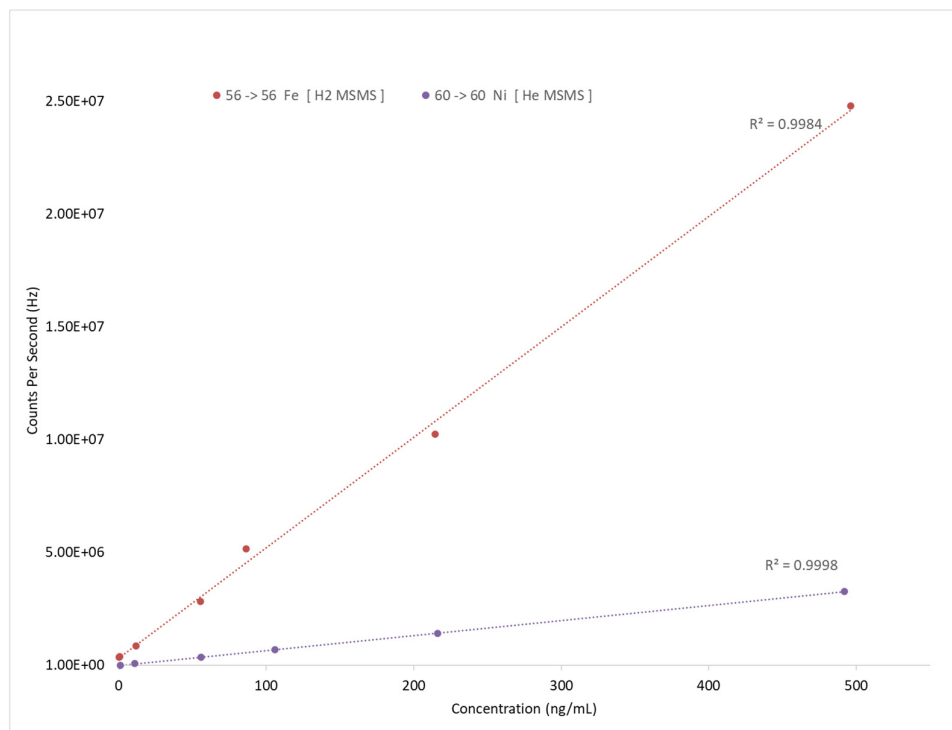
Figure S45. Plot of the calibration curves for the Ni and Fe atoms using 0, 1, 10, 50, 100, 200, and 500 ng/mL standard solutions.

Table S4. Concentrations of Fe and Ni obtained from the ICP-MS calibration curve.

[Fe] (ng/mL)	[Ni] (ng/mL)	[Fe] (µM)	[Ni] (µM)	[Fe]/[Ni]
278.645	285.092 ng/mL	5.000	4.857	1.027

Fe concentrations were obtained from H_2 MSMS and Ni concentrations from He MSMS.

35

Computational studies

Theoretical calculations were performed using the Gaussian16 computational package[3] using B3LYP[4-6] as the functional, def2-TZVP as the basis set for all non-metals and def2-TZVPP[7-8] for Ni and Fe for all calculations. Accuracy of this level of theory was evaluated by using the solid-state structure obtained from Xray crystallography as a standard and were deemed appropriate based on bond angles and distances of the optimized geometry. Frequency calculations were performed to confirm that the optimized geometry is at a minimum. Time dependent density functional theory calculations were performed on the structure optimized for the reduced compound with 25 allowed transitions in o-difluorobenzene ($\varepsilon = 14.3$) using the solvation model based on density.[9] The multiplicity of the systems was determined from the Evans method (Table S3).

Figure S46. Experimental and simulated spectra of (fc^{P,B})NiBr.

Figure S47. Experimental and simulated spectra of [(fc^{P,B})NiBr]$^+$.

Coordinates of (fc^P,B)NiBr

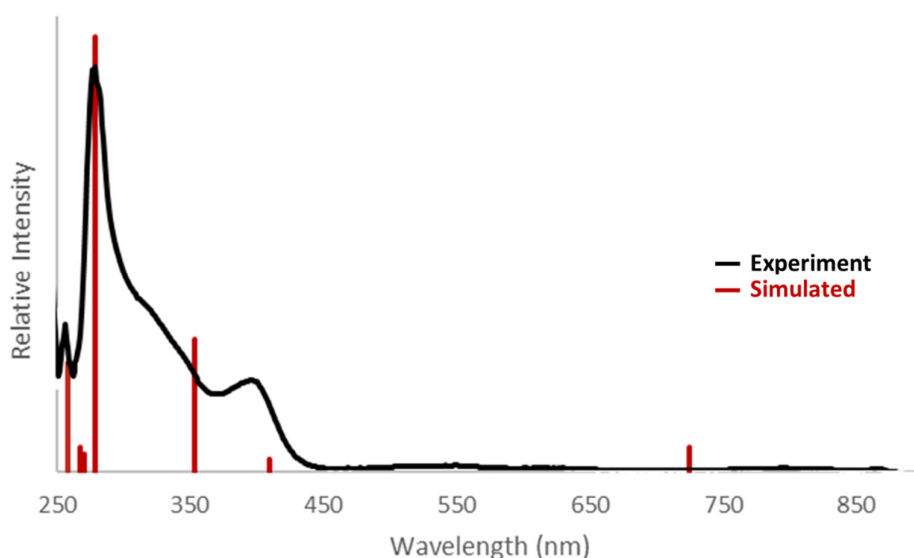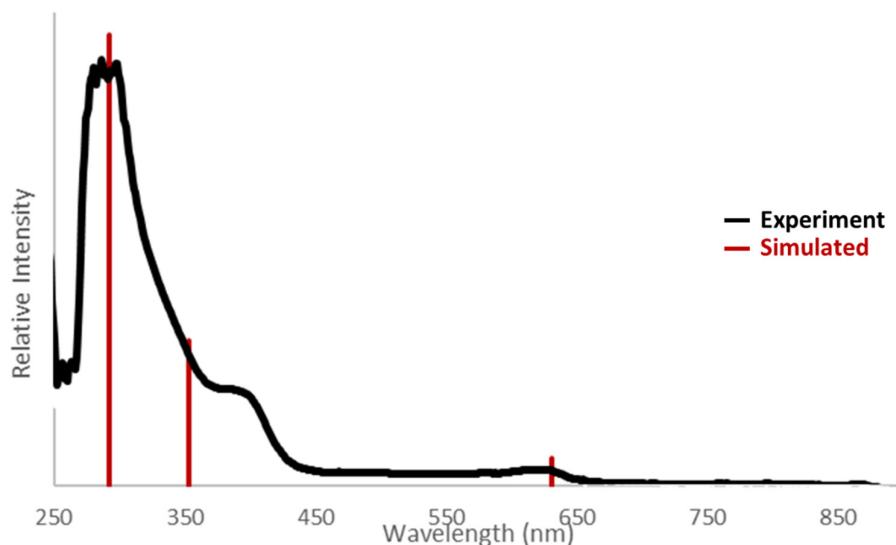|			
Br	1.738541000000	-3.436676000000	0.077183000000
Fe	-1.423854000000	2.570190000000	-0.375282000000
Ni	0.249076000000	-1.575785000000	-0.022238000000
P	1.448540000000	0.524365000000	0.055836000000
N	-2.310721000000	-1.060434000000	-1.476188000000
N	-0.974454000000	-1.316074000000	-1.592068000000
N	-1.194302000000	-1.565726000000	1.378330000000
N	-2.506627000000	-1.317941000000	1.081673000000
C	3.004290000000	0.521584000000	-0.925432000000
C	0.544417000000	1.944010000000	-0.597121000000
C	-0.123220000000	1.973111000000	-1.867658000000
H	-0.281289000000	1.127703000000	-2.515978000000
C	0.511454000000	3.277297000000	-0.068773000000
H	0.922134000000	3.588087000000	0.877597000000
C	-2.903684000000	-1.247364000000	-2.673823000000
C	3.236971000000	1.613318000000	1.974796000000
H	3.957677000000	1.696371000000	1.173005000000
C	-2.864945000000	1.075605000000	0.062962000000
C	-0.729435000000	-1.663964000000	-2.865768000000
C	1.409193000000	1.412030000000	4.058790000000
H	0.693959000000	1.327376000000	4.867475000000
C	1.972910000000	1.070642000000	1.729165000000
C	-0.161134000000	4.106100000000	-1.003131000000
H	-0.370632000000	5.156504000000	-0.876556000000
C	-3.401285000000	2.104332000000	-0.775259000000
H	-3.796246000000	1.959603000000	-1.769520000000
C	-1.923826000000	-1.624035000000	-3.583002000000
H	-2.064110000000	-1.855590000000	-4.625621000000
C	-1.151152000000	-2.134501000000	2.596227000000
C	-2.437698000000	1.743976000000	1.253918000000
H	-1.982585000000	1.264053000000	2.105485000000
C	3.342774000000	1.581801000000	-1.772497000000
H	2.678158000000	2.428158000000	-1.876023000000
C	1.065992000000	0.967481000000	2.787945000000
H	0.088957000000	0.537048000000	2.617754000000
C	3.881539000000	-0.562583000000	-0.814985000000
H	3.626088000000	-1.406339000000	-0.187319000000
C	-3.279656000000	-1.713946000000	2.113960000000
C	-4.367129000000	-1.084663000000	-2.924428000000
H	-4.954623000000	-1.767381000000	-2.308409000000
H	-4.577903000000	-1.299292000000	-3.971936000000
H	-4.715091000000	-0.074397000000	-2.706192000000
C	2.667918000000	1.955000000000	4.292907000000
H	2.937324000000	2.296407000000	5.284645000000
C	4.534423000000	1.558705000000	-2.488897000000
H	4.781567000000	2.386962000000	-3.141578000000
C	-0.544843000000	3.304543000000	-2.114038000000
H	-1.097720000000	3.639983000000	-2.977125000000
C	0.631783000000	-2.031842000000	-3.360540000000

H	1.346729000000	-1.216990000000	-3.224481000000
H	0.586610000000	-2.263091000000	-4.424455000000
H	1.027696000000	-2.900865000000	-2.832641000000
C	3.580664000000	2.051315000000	3.249102000000
H	4.564384000000	2.469416000000	3.423167000000
C	5.073716000000	-0.578568000000	-1.528638000000
H	5.739368000000	-1.427426000000	-1.434651000000
C	0.107703000000	-2.608780000000	3.245421000000
H	0.410664000000	-3.579777000000	2.849986000000
H	-0.049377000000	-2.708084000000	4.319909000000
H	0.939964000000	-1.925038000000	3.081974000000
C	5.403154000000	0.480316000000	-2.368038000000
H	6.329483000000	0.462494000000	-2.928962000000
C	-3.315759000000	3.361250000000	-0.111356000000
H	-3.626000000000	4.315243000000	-0.508737000000
C	-4.765786000000	-1.576316000000	2.149924000000
H	-5.077189000000	-0.532030000000	2.088760000000
H	-5.143114000000	-1.992792000000	3.083629000000
H	-5.237144000000	-2.104929000000	1.320222000000
C	-2.448507000000	-2.234705000000	3.095598000000
H	-2.748205000000	-2.644374000000	4.045720000000
C	-2.711080000000	3.136043000000	1.154696000000
H	-2.481806000000	3.886833000000	1.894741000000
B	-2.987651000000	-0.518554000000	-0.172489000000
H	-4.156305000000	-0.777767000000	-0.294779000000

References

1.   Stejskal, E. O.; Tanner, J. E., Spin diffusion measurements: spin echoes in the presence of a time-dependent field gradient. *J. Chem. Phys.* **1965,** *42* (1), 288-292.

2.   Abubekerov, M.; Diaconescu, P. L., Synthesis and Characterization of Ferrocene-Chelating Heteroscorpionate Complexes of Nickel(II) and Zinc(II). *Inorg. Chem.* **2015,** *54* (4), 1778–1784.

3.   Frisch, M. J.; Trucks, G. W.; Schlegel, H. B.; Scuseria, G. E.; Robb, M. A.; Cheeseman, J. R.; Scalmani, G.; Barone, V.; Petersson, G. A.; Nakatsuji, H.; Li, X.; Caricato, M.; Marenich, A. V.; Bloino, J.; Janesko, B. G.; Gomperts, R.; Mennucci, B.; Hratchian, H. P.; Ortiz, J. V.; Izmaylov, A. F.; Sonnenberg, J. L.; Williams; Ding, F.; Lipparini, F.; Egidi, F.; Goings, J.; Peng, B.; Petrone, A.; Henderson, T.; Ranasinghe, D.; Zakrzewski, V. G.; Gao, J.; Rega, N.; Zheng, G.; Liang, W.; Hada, M.; Ehara, M.; Toyota, K.; Fukuda, R.; Hasegawa, J.; Ishida, M.; Nakajima, T.; Honda, Y.; Kitao, O.; Nakai, H.; Vreven, T.; Throssell, K.; Montgomery Jr., J. A.; Peralta, J. E.; Ogliaro, F.; Bearpark, M. J.; Heyd, J. J.; Brothers, E. N.; Kudin, K. N.; Staroverov, V. N.; Keith, T. A.; Kobayashi, R.; Normand, J.; Raghavachari, K.; Rendell, A. P.; Burant, J. C.; Iyengar, S. S.; Tomasi, J.; Cossi, M.; Millam, J. M.; Klene, M.; Adamo, C.; Cammi, R.; Ochterski, J. W.; Martin, R. L.; Morokuma, K.; Farkas, O.; Foresman, J. B.; Fox, D. J. *Gaussian 16 Rev. A.03*, Wallingford, CT, 2016.

4.   Becke, A. D., Density-functional thermochemistry. III. The role of exact exchange. *J. Chem. Phys.* **1993,** *98* (7), 5648-5652.

5.   Lee, C.; Yang, W.; Parr, R. G., Development of the Colle-Salvetti correlation-energy formula into a functional of the electron density. *Phys. Rev. B* **1988,** *37* (2), 785.

6.   Stephens, P. J.; Devlin, F. J.; Chabalowski, C. F.; Frisch, M. J., Ab Initio Calculation of Vibrational Absorption and Circular Dichroism Spectra Using Density Functional Force Fields. *J. Phys. Chem.* **1994,** *98* (45), 11623-11627.

7.   Weigend, F.; Ahlrichs, R., Balanced basis sets of split valence, triple zeta valence and quadruple zeta valence quality for H to Rn: Design and assessment of accuracy. *Phys. Chem. Chem. Phys.* **2005,** *7* (18), 3297-3305.

8.   Schafer, A.; Huber, C.; Ahlrichs, R., Fully optimized contracted Gaussian basis sets of triple zeta valence quality for atoms Li to Kr. *J. Chem. Phys.* **1994,** *100* (8), 5829-5835.

9.   Marenich, A. V.; Cramer, C. J.; Truhlar, D. G., Universal Solvation Model Based on Solute Electron Density and on a Continuum Model of the Solvent Defined by the Bulk Dielectric Constant and Atomic Surface Tensions. *J. Phys. Chem.* **2009,** *113* (18), 6378-6396.